DEBRANCHING OF WAXY MAIZE STARCHES BY PULLULANASE, AND STRUCTURE AND DIGESTIBILITY OF SPHERULITES FORMED

by

JIALIANG SHI

B.S., Zhenghzou University of Light Industry, 2011

A THESIS

submitted in partial fulfillment of the requirements for the degree

MASTER OF SCIENCE

Department of Grain Science and Industry
College of Agriculture

KANSAS STATE UNIVERSITY
Manhattan, Kansas

2016

Approved by:

Major Professor
Yong-Cheng Shi

Abstract

Resistant starch (RS) is notable for having several health benefits in humans, including glucose control and intestinal well-being. Pullulanase is able to debranch amylopectin and result in higher RS content. Different levels of pullulanase have been used to debranch waxy maize starch in the literature, but the changes of structure during debranching are well documented. In this study, waxy maize starch was cooked and debranched by pullulanase with 80, 160 and 240 New Pullulanase Unit Novo (NPUN)/g starch pullulanase. One NPUN was defined as the amount of enzyme, which, under standard conditions, hydrolyzes pullulan, liberating reducing carbohydrate with reducing power equivalent to 1 µmole glucose per minute. The structure of waxy maize starch during debranching was investigated and the digestibility of the debranched products was measured. When pullulanase was increased from 80 to 240 NPUN/g, more amylopectin was debranched in the same debranching time, and the degree of crystallinity and the RS content increased. After the debranched starches were crystallized at 25°C for 24 hours, the RS contents were greater than 63%. When heated and recrystallized under highly regulated conditions, the linear material formed crystallites of a range of geometries, including spherulites of a highly organized structure. Debranched waxy maize starches were used to produce crystalline structure under four conditions: spherulites formed by adding ethanol and crystallized at 4°C (ES4); spherulites formed in water (WS4) at 4°C; particles formed at 50°C (WS50); and spherulites formed at 50°C then further precipitated at 4°C (WS50-4). Spherulites formed at 50°C (WS50) had a higher proportion of smaller molecules than existed in the parent starch (Rh<15nm). ES4 and WS4 were B-type crystalline structure; whereasWS50 and WS50-4 were A-type crystalline structure. ES4 had a larger proportion of molecules with a low degree of polymerization and the RS content was also the lowest of the four samples. With cooling from

50°C to 4°C (WS50-4), the RS content was increased from 60% to 73%. ES4 and WS50-4 contained particles with spherical symmetry and WS4 had partial radial symmetry with some distortions, whereas WS50 displayed oblate particles with a parallel crystal structure.

Table of Contents

List of Figures

List of Tables

Acknowledgements

The project was completed under the direction and guidance by Dr. Yong-Cheng Shi. He led me into starch research and gave me an opportunity to complete this thesis and work with other outstanding researchers. I am very appreciative of Dr. Shi's advice and encouragement on this thesis.

I also thank Dr. Michael Sweedman for his cooperation and expertise on the development of spherulites formation using the parr reactor and scientific writing.

Special thanks to Dr. Wilson and Dr. Dogan for their time and effort in serving on the advisory committee.

Chapter 1 - Introduction

In general starch contains two types of glucose polymers: amylose and amylopectin. Amylose consists of primarily linear molecules linked by α-1,4-glycosidic bonds, whereas amylopectin is highly branched molecule containing α-1,4-glycosidic and around 5% α-1,6-glycosidic bonds (Hizukuri, et al., 2006). Waxy maize starch contains essentially 100% amylopectin.

Starch naturally forms two main types of crystallites: type A and type B. A-type crystalline structure is observed in cereal starches, such as waxy maize starch, while B-type structure forms in tuber, root and amylose-rich starches (Bogracheva, et al. 1998). A-type crystalline structure is denser and formed as a monoclinic unit cell containing 4 water molecules (Imberty et al, 1988) whereas B-type crystalline structure is a hexagonal unit cell containing 36 water molecules (Imberty & Perez, 1988). In previous studies, short chain amylose (SCA) from debranched waxy maize starches was used to produce highly crystalline materials (Buléon et al, 2007; Cai & Shi, 2010; Cai et al, 2010; Gidley & Bulpin, 1987; Ring et al, 1987).

The type of crystalline structure is influenced by solvent, chain length, solid concentration and crystallization temperature. Generally, shorter chain length, higher concentration and crystallization temperature result in the formation of A-type crystallites, while the reverse conditions favors the formation of B-type of crystallites (Buléon et al., 2007; Cai & Shi, 2010; Cai et al., 2010; Gidley & Bulpin, 1987). When ethanol was added to enhance

crystallization of short chains, A-type of crystallites were observed during cooling (Helbert et al, 1993; Ring et al., 1987).

Resistant starch is the starch and its degraded products which resist to digestion and absorption in the small intestine. Resistant starch can be classified into five types. RS-I is physically inaccessible to the enzyme, RS-II includes raw starches of some plant species, RS-III is formed during retrogradation and is the main type of RS in this study, and RS-IV is chemically modified (Topping et al., 2003). RS-V refers to a complex formed from amylose and polar lipids (Hasjim et al., 2013).

When starch is heated in water, the organized structure of starch granules is destroyed and the process is called gelatinization. After subsequent cooling, linear regions of amylopectin and linear amylose become associated in a process called retrogradation, increasing their RS-III content. RS III is produced by crystallization of starch molecules, influenced by temperature, degree of polymerization (DP), solid concentration and solvent. The yield of RS III increases with higher DP (up to 100) of amylose (Eerlingen et al., 1993). Erlangen (1993) suggested that the average DP of RS was between 19 and 26, and two mechanisms of RS formation were suggested: (a) micelle formation with amylose; (b) lamellar structures formed by folding amylose chains. Some studies investigated the digestibility of pure A- and B-type crystals. Williamson et al. (1992) produced A- and B- type spherulites crystals and found B-type crystals were more resistant to the hydrolysis of α-amylase. In contrast, Cai et al. (2010) found A-type crystals formed from SCA were more resistant to enzyme digestion (Cai & Shi, 2010; Cai et al,

2010). As a result, the relationship between digestibility and crystalline type is not fully understood.

Spherulites have the properties of granular morphology and the crystalline types of native starch, which makes them a good model to study the digestibility of starch crystallites. The morphology of starch spherulites was influenced starch source, amylose content and crystallization conditions, such as crystallization temperature, solid concentration, cooling rate and solvent (Nordmark & Ziegler, 2002a, 2002b; Ring et al., 1987; Singh et al, 2010; Ziegler et al, 2003; Creek et al, 2006). In previous studies, the spherulites were produced in differential scanning calorimeter (DSC) pan, so the amount of production was limited and not enough for digestion experiment (Creek et al, 2006; Ziegler et al., 2003). Cai & Shi (2013) have increased the amount of production and investigated the digestibility. In this study, the morphology and digestibility of spherulites formed in different conditions were investigated.

In order to obtain a proper material for the formation of spherulites, waxy maize starch was debranched by three activity levels of pullulanase in this thesis. The objective was to determine the structure changes during debranching. After debranching, the structure and digestibility of crystallized material were investigated.

Another objective was to produce spherulites with the debranched material. A pressure reactor was used to produce spherulites. The effects of adding ethanol and the temperature on crystallization were investigated. The morphology of the crystalline products and the digestibility were also determined.

References

Bogracheva, T. Y., Morris, V. J., Ring, S. G., & Hedley, C. L. (1998). The granular structure of C-type pea starch and its role in gelatinization. *Biopolymers*, *45*, 323–332.

Buléon, A., Véronèse, G., & Putaux, J.-L. (2007). Self-association and crystallization of amylose. *Australian Journal of Chemistry*, *60*, 706–718.

Cai, L., & Shi, Y.-C. (2010). Structure and digestibility of crystalline short-chain amylose from debranched waxy wheat, waxy maize, and waxy potato starches. *Carbohydrate Polymers*, *79*, 1117–1123.

Cai, L., & Shi, Y.-C. (2013). Self-assembly of short linear chains to A- and B-type starch spherulites and their enzymatic digestibility. *Journal of Agricultural and Food Chemistry*, *61*, 10787−10797.

Cai, L., Shi, Y.-C., Rong, L., & Hsiao, B. S. (2010). Debranching and crystallization of waxy maize starch in relation to enzyme digestibility. *Carbohydrate Polymers*, *81*, 385–393.

Creek, J. A., Ziegler, G. R., & Runt, J. (2006). Amylose crystallization from concentrated aqueous solution. *Biomacromolecules*, *7*, 761–770.

Eerlingen, R. C., Deceuninck, M., & Delcour, J. A. (1993). Enzyme-resistant starch. II. Influence of amylose chain length on resistant starch formation. *Cereal Chemistry*, *70*, 345–350.

Gidley, M. J., & Bulpin, P. V. (1987). Crystallisation of malto-oligosaccharides as models of the crystalline forms of starch: minimum chain-length requirement for the formation of double helices. *Carbohydrate Research*, *161*, 291–300.

Helbert, W., Chanzy, H., Planchot, V., Buléon, A., & Colonna, P. (1993). Morphological and structural features of amylose spherocrystals of A-type. *Int. J. Biol. Macromol.*, *15*, 183–187.

Hizukuri, S., Abe, J., & Hanashiro, I. (2006). Starch: Analytical aspects. In *Carbohydrates in food* (2nd ed, pp. 305–391). Boca Raton, FL: Taylor & Francis Group.

Hasjim, J., Ai, Y., & Jane, J. (2013). Novel applications of amylose-lipid complex as resistant starch type 5. In Yong-Cheng Shi and Clodualdo C. Maningat (eds.). *Resistant Starch: Sources, Applications and Health Benefits* (First Edition., pp. 79–94). The Atrium, Southern Gate, Chichester, West Sussex, UK: John Wiley & Sons, Ltd.

Imberty, A., Chanzy, H., Perez, S., Buléon, A., & Tran, V. (1988). The double-helical nature of the crystalline part of A-starch. *Journal of Molecular Biology*, *201*, 365–378.

Imberty, A., & Perez, S. (1988). A revisit to the three-dimensional structure of B-type starch. *Biopolymers*, *27*, 1205–1221.

Miao, M., Jiang, B., & Zhang, T. (2009). Effect of pullulanase debranching and recrystallization on structure and digestibility of waxy maize starch. *Carbohydrate Polymers*, *76*, 214–221.

Nordmark, T. S., & Ziegler, G. R. (2002a). Spherulitic crystallization of gelatinized maize starch and its fractions. *Carbohydrate Polymers*, *49*, 439–448.

Nordmark, T. S., & Ziegler, G. R. (2002b). Structural features of non-granular spherulitic maize starch. *Carbohydrate Research*, *337*, 1467–1475.

Ring, S. G., Miles, M. J., Morris, V. J., & Turner, R. (1987). Spherulitic crystallization of short chain amylose. *Int. J. Biol. Macromol.*, *9*, 158–160.

Shi, M., Chen, Y., Yu, S., & Gao, Q. (2013). Preparation and properties of RS III from waxy maize starch with pullulanase. *Food Hydrocolloids*, *33*, 19–25.

Shi, Y. C., & Maningat, C. C. (2013). *Resistant Starch, Sources, Applications and Health*. IFT Press, Wiley Blackwell.

Singh, J., Lelane, C., Stewart, R. B., & Singh, H. (2010). Formation of starch spherulites: Role of amylose content and thermal events. *Food Chemistry*, *121*, 980–989.

Topping, D., Fukushima, M., & Bird, A. R. (2003). Resistant starch as a prebiotic and synbiotic: state of the art. *Proceedings of Nutrition Society*, *62*, 171–176.

Williamson, G., Beishaw, N. J., Self, D. J., Ring, S. G., Cairns, P., Morris, V. J., and Parker, M. L. (1992). Hydrolysis of A-type and B-type crystalline polymorphs of starch by Alpha-amylase, Beta-amylase and Glucoamylase-1. *Carbohydrate Polymers*, *18*, 179–187.

Ziegler, G. R., Nordmark, T. S., & Woodling, S. E. (2003). Spherulitic crystallization of starch: influence of botanical origin and extent of thermal treatment. *Food Hydrocolloids*, *17*, 487–494.

Zobel, H. F. (1988). Starch crystal transformations and their industrial importance. *Starch - Stärke*, *40*, 1–7.

Chapter 2 - Effects of pullulanase activity on debranching of waxy maize starch and digestibility of debranched products.

Introduction

Waxy maize starch consists almost entirely of amylopectin. Branches in amylopectin are connected by α-1,6-glycosidic bonds, which like α-1,4 bonds can be hydrolyzed by acids or enzymes. Those α-1,6-glycosidic bonds can be cleaved by debranching enzymes such as isoamylase and pullulanase (Manners, 1989). When these debranching enzymes are applied to waxy starches, large amylopectin molecules are broken into short linear chains. Both isoamylase and pullulanase have been used for examination of chain profile (Akai et al., 1971; Lee et al., 1968). However, these two debranching enzymes have different reaction patterns (Hizukuri et al, 2006; Manners & Matheson, 1981; Yokobayashi et al, 1973). Pullulanase shows a slow exo-wise action (Hizukuri et al., 2006), whereas isoamylase hydrolyze both inner and outer branches on amylopectin (Manners & Matheson, 1981; Yokobayashi et al., 1973).

Berry (1986) used pullulanase to increase resistant starch (RS) content in waxy maize starch to 33%. However, the structure of debranched starches was not analyzed. Using isoamylase, Shi et al. (2006) debranched low-amylose starches and produced products with greater than 70% RS content. Miao et al. (2009) used pullulanase to debranch waxy maize starch and the RS contents was less than 50%. In their experiment, debranched starch precipitation was facilitated by adding ethanol, which resulted in lower RS content (Evans & Thompson,

2008).The influence of different concentrations of pullulanase on debranching of waxy maize starch was investigated by Shi et al. (2013). They used five different concentrations of pullulanase from 5 to 30 ASPU/g (ASPU is defined as the amount of enzyme that liberates 1.0 mg glucose from starch in 1 min at pH 4.4 and 60°C) to hydrolyze waxy maize starch for 24 hours. However, the changes of structure during debranching was not investigated. Sun et al. (2014b) used pullulanase (30ASPU/g) to debranched waxy maize starch. The yields and degree of crystallinity of debranched material were investigated, but the resistant starch content was unknown. Sun et al. (2014a) also investigated the influence of retrogradation time on crystallinity of proso millet starch. The yields were low (less than 60%), and because not all debranched materials were collected, the structure of debranched starches was unknown.

Reviewing previous work in the literature reveals that the structural changes of starch during the debranching of starch by pullulanase are not well documented. The reported RS content was lower than 50% RS content when pullulanase was used to debranch waxy maize starch. There is a need to understand how the structure of starch changes during the debranching by pullulanase because the commercial availability of isoamylase is limited. In the current study, the first objective was to investigate the efficiency of pullulanase on debranching of waxy maize starch, and the second objective was to produce debranched starch with a high RS content.

Materials and Methods

Materials

Waxy maize starch (Amioca) was obtained from Ingredion Inc. (Bridgewater, NJ). Pullulanase (Promozyme D6, 4000 NPUN/g) was obtained from Novozyme (Franklinton, NC). One pullulanase unit (NPUN) was defined as the unit amount of enzyme that hydrolyzes pullulan under standard conditions (pH=5, 40°C, incubation of 20 min) and liberates 1 μmole of reducing carbohydrate per minute (Svendsen, et al. 2004). Isoamylase (EC 3.2.1.68) was obtained from Sigma, and the activity was 7421000 units/mg. One unit causes an increase in absorbance at 610 nm of 0.1 in 1 hour using rice starch as a substrate. An α-amylase assay kit was purchased from Megazyme Inc. (Wicklow, Ireland). Other chemicals were analytical grade.

Debranching starch

Waxy maize starch (100g, db) was mixed with 300 g de-ionized water in a pressure bottle (1L, ACE glass, Vineland, USA). The mixture had a pH of 6 and was heated in a boiling water bath for 30 minutes with a magnetic stirring bar. The mixture was then heated in an oven at 120°C for 30 minutes. The slurry was transparent after heating. When the mixture was cooled to 60°C, pullulanase (40, 80, 160 and 240 NPUN/g) was added and the mixture was incubated in a water bath at 60°C and maintained at 60°C for 24 hours with constant shaking. After incubation, the mixture was placed at 25°C for 24 hours. The yields of crystalline precipitate at different time points were determined by centrifuging the mixture and subtracting the soluble carbohydrate

content as determined with a portable refractometer (Fisher Scientific Inc., Pittsburgh, PA, USA). The slurry was filtered with a funnel containing a piece of filter paper, and the cake was dried in an oven at 40°C overnight (Cai, Shi, Rong, & Hsiao, 2010; Cai & Shi, 2010). The dried starch was weighed and used to calculate the yields.

In other experiments, the starch was debranched with 80,160 or 240 NPUN/g of pullulanase and collected at following time points: 1, 2, 4, 8, 16, and 24 hours. Samples were freeze-dried and molecular size distributions were determined by gel permeation chromatography (GPC).

Assay for α-amylase activity in Pullulanase

The activity of α-amylase in pullulanase was measured by AOAC method 2002.01. using a Megazyme Kit (K-CERA 01/12). Standard flour sample and chemicals were from the same Megazyme Kit. The activity unit of α-amylase is Ceralpha Unit (CU), where CU is defined as the amount of enzyme required to release one micromole of p-nitrophenol from non-reducing-end blocked p-nitrophenyl maltoheptaoside in one minute under the defined assay conditions.

Reducing ends determination

Average degree of polymerization was determined by the Nelson/Somogyi reducing sugar method (McCleary, 1999; Nelson, 1944; Somogyi, 1952).

Debranched starch was dissolved in water (1mg/ml) and placed in a boiling water bath for 1 hour, then 0.5 ml sample solution was mixed with 0.5 ml cooper regent and placed in a

boiling water bath for 20 min, then the sample was cooled to ambient temperature (~25°C) for 5 min. Arsenomolybdate regent (3 ml) was added at room temperature and the absorbance measured at 520 nm after 10 min. Glucose solutions were used as standards.

Gel permeation chromatography (GPC)

From each sample, 4 mg of solid was dissolved in 4 ml of dimethyl sulfoxide (DMSO) (HPLC grade) containing lithium bromide (0.5% w/w) (Vilaplana & Gilbert, 2010). The mixture was tightly sealed and stirred in a boiling water bath for 24 hours, cooled to 25°C, filtered through a 0.45 μm filter and then injected into a PL-GPC 220 instrument (Polymer Laboratories, Inc., Amherst, MA, USA) equipped with three Phenogel columns (Cai et al., 2010) (Phenomenex, Inc., Torrance, CA, USA) and a guard column (Phenomenex, Inc., Torrance, CA, USA). The eluent was DMSO containing 0.5% (w/w) LiBr, and the flow rate was 0.8 mL/min. Temperature was controlled at 80°C. Pullulan standards were used for universal calibration (Vilaplana & Gilbert, 2010). The results of GPC were presented with the terms of hydrodynamic radius (R_h), whit $V_h = 4/3\pi R_h^3$.

High-performance anion exchange chromatography (HPAEC)

The chain length distributions (CLD) of starch were measured by HPAEC (Dionex ICS-3000, Dionex Corp., Sunnyvate, CA, USA), equipped with a pulsed amperometric detector, a guard column, a CarboPacTM PA1 analytical column and an AS-DV autosampler (Cai et al., 2010b). Starch (5 mg) was dissolved in 5 ml of water in a boiling water bath for 1 h with stirring.

The eluents were prepared as described previously (Shi & Seib, 1992). Eluent A was 150 mM NaOH, and eluent B was 150 mM NaOH containing 500 mM sodium acetate. The gradient program used eluent B in the proportions: 40, 50, 60, and 80% at 0, 2, 10, and 40 min, respectively. The separations were carried out at 25°C and the flow rate was 1 ml/min.

To prepare a completely debranched starch, waxy maize starch (20 mg db) was heated in 10 ml of de-ionized water for 1 hour in a boiling water bath. The mixture was cooled to 50°C, and isoamylase (1%, w/w) was added. The starch was debranched for 12 hours. The debranched starch was freeze dried and its CLD was determined by HPAEC.

X-ray diffraction (XRD)

The moisture of samples was adjusted to about 17% in a sealed desiccator containing water at the bottom at 25°C before analysis. The types of crystalline structure of debranched starch were determined by wide-angle X-ray diffraction (PANalytical, Almelo, The Netherlands). The measurements were conducted at 35 kV and 20 mA with a theta-compensating slit and a diffracted beam monochromator. The diffractograms were recorded between 2 and 35° (2θ). Relative degree of crystallinity was calculated by the ratio of the peaks representing crystals as a proportion of the amorphous area (Komiya & Nara, 1986).

Digestibility of debranched starches

A modified Englyst method was used (Englyst et al., 1992; Sang & Seib, 2006). Samples were digested by pancreatin and amyloglucosidase, then 4 ml of the digested sample solution

was transferred into 20 ml of ethanol after 20, 40, 60, 80, 120 and 240 min. The precipitates at each time point were collected and measured by differential scanning calorimetry (DSC).

Differential scanning calorimetry (DSC)

Each sample (4 mg, db) was loaded in a DSC stainless pan. Water (12µl) was added and the pan was sealed. An empty pan was used as a reference. Samples were measured with a TAQ5000 (TA Instruments, New Castle, DE, USA) and heated from 10 to 160°C with a heating rate of 10°C/min. The onset, peak, conclusion temperatures (T_o, T_p, and T_c respectively) and enthalpy were calculated from the DSC thermogram.

Statistical analysis

The analyses of variance (ANOVA) mean values were determined by Minitab 17 Statistical Software Program (Minitab Inc. State College PA, USA). Values are not significantly different when the p-value is larger than 0.05. Experiments were run in duplicate, and mean value and standard deviation were reported.

Results and Discussion

Molecular size distribution

Molecular size distribution of debranched waxy maize starches was shown in Figure 2.1. After adding pullulanase (80, 160 and 240 NPUN/g), two major peaks were detected. The first peak appearing at Rh=1 nm represents the unit chains released by debranching whereas the

second peak appearing after Rh=7 nm represents branched molecules. Starch debranched by 80 NPUN/g of pullulanase had a larger peak at Rh=10 nm and its molecular size range was larger. Starch treated by 240 NPUN/g of pullulanase had the narrowest range of molecule sizes and its second peak was smaller. The percentage of debranched starch was obtained by the ratio of first peak area to the total peaks area (Figure 2.2). Higher pullulanase activity resulted in a higher level of debranched starch at the same debranching time and starch was debranched faster in the first two hours. The debranching rate of the sample treated by 80 NPUN/g of pullulanase was linear after two hours; whereas the debranching rates of the sample treated by 160 and 240 NPUN/g of pullulanase were relatively lower between 2 and 16 hours, and then the debranching rates were slightly changed after 16 hours. After 24 hours, the waxy maize starches treated by 80, 160 and 240 NPUN/g pullulanase were 66.4, 75.8 and 82.8% debranched respectively. When the starch was treated by 40 NPUN/g of enzyme for 24 hours, the resulted debranched starch was still a gel and difficult to recover. The second peak was much larger after 24 hours compared to 80-240 NPUN/g of pullulanase samples. As a result, this sample was not used for other measurements.

In a previous study, waxy maize starches were hydrolyzed with isoamylase (Cai et al., 2010). Isoamylase is able to hydrolyze both inner and outer branching linkages, whereas pullulanase is thought to hydrolyze outer branches (Harada et al., 1972). Compared to the rate of pullulanase on hydrolysis of α-(1,6) linkages of amylopectin, the rate of isoamylase is 7 times faster (Robyt, 2009).

Yields

After 24 hours, the starch treated by 80, 160 and 240 NPUN/g of pullulanase became white precipitates, but the sample treated by 40 NPUN/g of pullulanase still contained starch gel, which made the calculation of precipitate yield difficult. Changing the level of pullulanase did not obviously changed the yield curve, so only the yield of sample debranched by 80 NPUN/g of pullulanase was shown in Figure 2.3. The yield of precipitate was only 41% after 24 hours of incubation at 60°C. However, after cooling to 25°C, the yield was increased rapidly to 73.3% in the first 1.5 hours and then the rate of precipitation was decreased. Starch debranched by 80, 160 and 240 NPUN/g of pullulanase had the similar yield (85-87%) during crystallization (Table 2.1).

Crystallization occurred as soon as short linear molecules (DP about 6-80) were released (Cai et al., 2010a). The formation of double helices requires a degree of polymerization (DP) of greater than 10 (Gidley & Bulpin, 1987b), and the maximum RS content was obtained when DP was about 100 (Eerlingen et al., 1993). Shi and Jeffcoat (2011) also reported that enzyme resistant crystallized molecules had ranging from 30 to 65. Amylose may form random coils with single helices in aqueous solution (Ring et al., 1985), and these single helices can further associate to form double helices, which results into crystallites and aggregates (Gidley, 1989).

Chain length distribution (CLD)

Chromatograms of the debranched starches are shown in Figure 2.4. In the samples debranched less than 8 hours, many peaks had a shoulder peak and the number of shoulder peaks appear to increase with more debranching time in samples treated by 80 and 160 NPUN/g of pullulanase, and after 8 hours, those shoulder peaks were decreased. However, the shoulder peaks were high in sample treated by 240 NPUN/g of pullulanase after 1 hour of debranching and more obvious at 24 hours. In addition, with longer debranching time, more peaks were detected after 15 min of retention time (Figure 2.4). After 24 hours debranching, most molecules were short chains (DP6-36), and few chains were longer than DP 60 (Figure 2.5).

After the debranched starch was recovered by filtration, the average DP was decreased with increasing pullulanase level (Table 2.2) indicating that more branches were released by increasing pullulanase level and this result matched with result of debranching degree (Figure 2.2). The CLD of fully debranched waxy maize starch (DWMS) treated by isoamylase was measured and compared to the treatment of pullulanase (Figure 2.5). DWMS contained relatively more molecules of DP 10-12; and the sample treated by 240 NPUN/g of pullulanase contained more molecules of DP 11-16 when compared to the samples treated by 80 and 160 NPUN/g of pullulanase. The CLD of DWMS was the same as previous studies (Bertoft & Mäkelä, 2006; Cai & Shi, 2010).

After 24 hours, the shoulder peaks were still observed (Figure 2.4), and with higher levels of pullulanase, those shoulder peaks became more evident. The increased number of shoulder

peaks is probably caused by α-amylase activity in pullulanase. The activity of α-amylase in the enzyme was 6.3 CU/g. This pullulanase contained a trace amount of α-amylase, which was able to hydrolyze α-1,4-linkages at either side of the α-1,6-linkages (Smirnova et al., 2015). However, pullulanase requires that each of the two chains connected by an α-1,6-glycosidic bond contains no less than two α-1,4-linked glucose units (Norman, 1982). As a result, the presence of α-amylase had an influence on debranching and has resulted in small branched molecules.

X-ray diffraction

The degree of crystallinity of debranched starches was increased with longer debranching time (Figure 2.6). Products treated with 80 NPUN of pullulanase had a low degree of crystallinity than products treated with higher levels of pullulanase throughout the debranching process (Table 2.3).

In the early stages of hydrolysis (less than 4 h), the amount of debranched starch was relatively small (Figure 2.2) and the branched, gelatinized starch did not readily form crystals. After higher levels of pullulanase activity cleaved more branches in the first 16 h of debranching (Figure 2.2), a higher level of crystallinity in samples treated by 240 NPUN/g of pullulanase was detected (Table 2.3). Between 2 and 8 h, the degree of crystallinity of the samples treated by 240 NPUN of pullulanase increased fastest, and then reached 57.2% crystallinity at 8 h. Further crystallization only increased crystallinity slightly to 62% at 24 h.

Samples treated with 160 and 240 NPUN of pullulanase (sample P160 and P240) started to show a B-type diffraction pattern after 4 h, whereas a B-type pattern was only detected after 8 hours in sample treated with 80 NPUN/g (P80) (Figure 2.6). Native waxy maize starch gave an A-type diffraction pattern (Figure 2.6). After debranching, short linear molecules are re-crystallized by cooling, and the type of crystallinity can be influenced by chain length (Cai & Shi, 2010). When waxy maize starch was debranched, most molecules were larger than DP 13, so B-type crystallinity was produced during crystallization (Figure 2.6), which is in agreement with previous work (Cai & Shi, 2010, Cai et al., 2012). However, A-type crystallites were also observed when debranched waxy maize starches (50% w/w) were melted by heating and then cooling to low temperature (25°C) at 10°C/min (Cai et al, 2012), possibly due to the high solid concentration during heat treatment.

Digestion

Increasing the level of pullulanase decreased RDS content (Table 2.4). After 240 min of digestion, the amounts of digested starch of three samples treated by different levels of pullulanase became very different (Figure 2.7). All debranched starches had a RS content greater than 60%, and the RS content in P240 was 70.7% (Table 2.4).

Resistant starch content was low in waxy maize starch, but was increased to 33% by the treatment of pullulanase (Berry, 1986). RS content may be increased with a higher level of pullulanase treatment (Shi et al. 2013, Shi & Gao, 2011 and Pongjanta et al. 2009). Miao et al.

(2009) used Englyst's method to measured RS content in debranched waxy maize starch treated by pullulanase. In their study, ethanol was used to facilitate precipitation. Ethanol precipitation of branched molecules may result into a low RS content (Evans & Thompson, 2008), so the RS contents were not higher than 50% (Miao et al. 2009). In contrast, when waxy maize starch was debranched by 1% isoamylase, the RS content in the precipitate was 86%, because waxy maize starch was completely debranched and readily crystallized (Cai et al., 2010).

To understand the mechanism of digestion of the debranched starches, undigested resistant residues of P80 after each time point of digestion were collected and analyzed by DSC (Table 2.5). The onset temperature was increased slightly after digestion. Interesting, the changes in ΔH were not great, indicating that both amorphous and crystalline regions were digested.

Conclusions

The effect of pullulanase content on the properties of debranched waxy maize starch and the structure changes during debranching were investigated. When the activity of pullulanase was 80 NPUN/g, 66.4% of waxy maize starches were debranched. With increasing pullulanase activity, more starch was debranched, and the portion of small DP molecules was also slightly increased. The RS content in sample treated by 80 NPUN/g of pullulanase was higher than 60%. When the activity of pullulanase was increased, the RS content and degree of crystallinity were

higher and the crystals were formed faster. Starch with high RS content could be produced by debranching waxy maize starches with pullulanase.

References

Akai, H., Yokobayashi, K., Misaki, A., & Harada, T. (1971). Structural analysis of amylopectin using Pseudomonas isoamylase. *Biochimica et Biophysica Acta*, *252*, 427–431.

Berry, C. S. (1986). Resistant starch: Formation and measurement of starch that survivs exhasutive digestion with amylolytic enzyme during the determination of dietary fiber. *Journal of Cereal Science*, *4*, 301–314.

Bertoft, E. (2015). Fine structure of amylopectin. In Yasunori Nakamura (Ed.). *Starch Metabolism and Structure* (illustrated, pp. 3–40). Springer Japan.

Bertoft, E., & Mäkelä, J. (2006). Structure of limit dextrins from storage polysaccharides: A comparsion between amylopectin and glucogen. In Vladimir P. Yuryev, Piotr Tomasik, and Eric Bertoft (Eds.). *Starch: Achievements in Understanding of Structure and Functionality* (pp. 87–105). New York: Nova Publishers.

Bird, A. R., Lopez-Rubio, A., Shrestha, A. K., & Gidley, M. J. (2009). Resistant starch in vitro and in vivo: factors determining yield, structure, and physiological relevance. In Stefan Kasapis, Ian Norton, Johan Ubbink (Ed.). *Modern Biopolymer Science* (pp. 449–510). London, United Kingdom: Academic Press, Elsevier Inc.

Buléon, A., Véronèse, G., & Putaux, J.-L. (2007). Self-association and crystallization of amylose. *Australian Journal of Chemistry*, *60*, 706–718.

Cai, L., Bai, Y., & Shi, Y.-C. (2012). Study on melting and crystallization of short-linear chains from debranched waxy starches by in situ synchrotron wide-angle X-ray diffraction. *Journal of Cereal Science*, *55*, 373–379.

Cai, L., & Shi, Y.-C. (2010). Structure and digestibility of crystalline short-chain amylose from debranched waxy wheat, waxy maize, and waxy potato starches. *Carbohydrate Polymers*, *79*, 1117–1123.

Cai, L., Shi, Y.-C., Rong, L., & Hsiao, B. S. (2010). Debranching and crystallization of waxy maize starch in relation to enzyme digestibility. *Carbohydrate Polymers*, *81*, 385–393.

Eerlingen, R. C., Deceuninck, M., & Delcour, J. A. (1993). Enzyme-resistant starch. II. Influence of amylose chain length on resistant starch formation. *Cereal Chemistry*, *70*, 345–350.

Eerlingen, R. C., & Delcour, J. A. (1995). Formation, analysis, structure and properties of type III: Enzyme Resistant Starch. *Journal of Cereal Science*, *22*, 129–138.

Englyst, H. N., Kingman, S. M., & Cummings, J. H. (1992). Classification and measurement of nutritionally important starch fractions. *European Journal of Clinical Nutrition*, *46*, S33–S50.

Englyst, K. N., Liu, S., & Englyst, H. N. (2007). Nutritional characterization and measurement of dietary carbohydrates. *European Journal of Clinical Nutrition*, *61*, S19–S39.

Evans, A., & Thompson, D. B. (2008). Enzyme susceptibility of high-amylose starch precipitated from sodium hydroxide dispersions. *Cereal Chemistry*, *85*, 480–487.

Gidley, M. J. (1989). Rheological studies of aqueous amylose gels: the effect of chain length and concentration on gel modulus. *Macromolecules*, *22*, 351–358.

Gidley, M. J., & Bulpin, P. V. (1987). Crystallisation of malto-oligosaccharides as models of the crystalline forms of starch: minimum chain-length requirement for the formation of double helices. *Carbohydrate Research*, *161*, 291–300.

Hanashiro, I. (2015). Fine Structure of Amylose. In Yasunori Nakamura (Ed.). *Starch Metabolism and Structure* (illustrated, pp. 41–60). Springer Japan.

Harada, T., Misaki, A., Akai, H., Yokobayashi, K., & Sugimoto, K. (1972). Characterization of Pseudomonas isoamylase by its actions on amylopectin and glycogen: Comparison with Aerobacter pullulanase. *Biochimica et Biophysica Acta (BBA) - Enzymology*, *268*, 497–505.

Hasjim, J., Ai, Y., & Jane, J. (2013). Novel applications of amylose-lipid complex as resistant starch type 5. In Yong-Cheng Shi and Clodualdo C. Maningat (eds.). *Resistant Starch: Sources, Applications and Health Benefits* (First Edition., pp. 79–94). The Atrium, Southern Gate, Chichester, West Sussex, UK: John Wiley & Sons, Ltd.

Haub, M. D. (2013). Resistant starch on glycemia and satiety in humans. In Yong-Cheng Shi and Clodualdo C. Maningat (eds.). *Resistant Starch: Sources, Applications and Health Benefits* (First edition, pp. 207–214). The Atrium, Southern Gate, Chichester, West Sussex, UK: John Wiley & Sons, Ltd.

Hizukuri, S., Abe, J., & Hanashiro, I. (2006). Starch: Analytical aspects. In A.-C. Eliasson (Ed.), *Carbohydrates in food* (2nd ed, pp. 305–391). Boca Raton, FL: Taylor & Francis Group.

Jane, J. (2004). Starch: Structure and properties. In Piotr Tomasik (Ed.). *Chemical and Functional Properties of Food Saccharides* (illustrated, pp. 81–100). 2000 N.W. Corporate Blvd., Boca Raton, Florida: CRC Press.

Komiya, T., & Nara, S. (1986). Changes in crystallinity and gelatinization phenomena of potato starch by acid treatment. *Starch/Stärke*, *38*, 9–13.

Lee, E. Y. C., Mercier, C., & Whelan, W. J. (1968). A method for the investigation of the fine structure of amylopeclin. *Archives of Biochemistry and Biophysics*, *125*, 1028–1030.

Manners, D. J. (1989). Recent developments in our understanding of amylopectin structure. *Carbohydrate Polymer*, *11*, 87–112.

Manners, D. J., & Matheson, N. K. (1981). The fine structure of amylopectin. *Carbohydrate Research*, *90*, 99–110.

McCleary, B. V. (1999). Enzyme purity and activity in fiber determinations. *Cereal Foods World*, *44*, 590–596

Miao, M., Jiang, B., & Zhang, T. (2009). Effect of pullulanase debranching and recrystallization on structure and digestibility of waxy maize starch. *Carbohydrate Polymers*, *76*, 214–221.

Nelson, N. (1944). A photometriic adaptation of the Somogyi method for the determination of glucose. *Journal of Biological Chemistry*, *153*, 375–380.

Norman, B. E. (1982). A novel debranching enzyme for application in glucose syrup industry. *Starch-Stärke*, *34*, 340–346.

Pongjanta, J., Utaipattanaceep, A., Naivikul, O., & Piyachomkwan, K. (2009). Debranching enzyme concentration effected on physicochemical properties and α-amylase hydrolysis rate of resistant starch type III from amylose rice starch. *Carbohydrate Polymers*, *78*, 5–9.

Ring, S. G., L'Anson, K., & Morris, V. J. (1985). Static and dynamic light scattering studies of amylose solutions. *Macromolecules*, *18*, 182–188.

Robyt, J. N. (2009). Enzymes and Their Action on Starch. In *Starch Chemistry and Technology* (third edition, pp. 237–292). 30 Corporate Drive, Suite 400, Burlington, MA 01803, USA: Academic Press is an imprint of Elsevier.

Sang, Y., & Seib, P. A. (2006). Resistant starches from amylose mutants of corn by simultaneous heat-moisture treatment and phosphorylation☆. *Carbohydrate Polymers*, *63*, 167–175.

Shi, M., Chen, Y., Yu, S., & Gao, Q. (2013). Preparation and properties of RS III from waxy maize starch with pullulanase. *Food Hydrocolloids*, *33*, 19–25.

Shi, M., & Gao, Q. (2011). Physicochemical properties, structure and in vitro digestion of resistant starch from waxy rice starch. Carbohydrate Polymers, 84, 1151–1157.

Shi, Y.-C., Cui, X., Birkett, A. M., & Thatcher, M. G. (2006). Resistant starch prepared by isoamylase debranching of low amylose starch. Pat. No. 7 081 261.

Shi, Y.-C., & Jeffcoat, R. (2011). Structural Feature of Resistant Starch. In McCleary Barry V. and Prosky Leon (Eds.). *Advanced Dietary fibre Technology* (pp. 430–439). Osney Mead, Oxford: Blackwell Science.

Shi, Y.-C., & Seib, P. A. (1992). The structure of four waxy starches related to gelatinization and retrogradation. *Carbohydrate Research*, *227*, 131–145.

Shukri, R., Seib, P. A., Maningat, C. C., & Shi, Y.-C. (2013). In vitro enzymatic testing method and digestion mechanism of cross-linked wheat starch. In Yong-Cheng Shi and Clodualdo C. Maningat (eds.). *Resistant Starch: Sources, Applications and Health Benefits* (First edition, pp. 145-166). The Atrium, Southern Gate, Chichester, West Sussex, UK: John Wiley & Sons, Ltd.

Smirnova, J., Fernie, A. R., & Steup, M. (2015). Starch degradation. In Yasunori Nakamura (Ed.). *Starch Metabolism and Structure* (First edition, pp. 239–290). Springer Japan.

Somogyi, M. (1952). Notes on sugar determination. *Journal of Biological Chemistry*, *195*, 19-23.

Sun, Q., Gong, M., Li, Y., & Xiong, L. (2014a). Effect of retrogradation time on preparation and characterization of proso millet starch nanoparticles. *Carbohydrate Polymers*, *111*, 133–138

Sun, Q., Li, G., Dai, L., Ji, N., & Xiong, L. (2014b). Green preparation and characterisation of waxy maize starch nanoparticles through enzymolysis and recrystallisation. *Food Chemistry*, *162*, 223–228.

Svendsen, A., Andersen, C., & Borchert, T. (2004). Pullulanase variants and methods for preparing such variants with predetermined properties. Pat. No. US20040048247 A1

Topping, D., Fukushima, M., & Bird, A. R. (2003). Resistant starch as a prebiotic and synbiotic: state of the art. *Proceedings of Nutrition Society*, *62*, 171–176.

Vilaplana, F., & Gilbert, R. G. (2010). Two-dimensional size/branch length distributions of a branched polymer. *Macromolecules*, *43*, 7321–7329.

Yokobayashi, K., Akai, H., Sugimoto, K., & Harada, T. (1973). Comparison of kinetic parameters of Pseudomonas isoamylase and Aerobacter pullulanase. *Biochimica et Biophysica Acta*, *293*, 197–202.

Table 2.1 Yield of waxy maize starches debranched by different levels of pullulanase at 60°C and crystallized at 25°C for 24 h.

Enzyme level (NPUN/g)	Yields (%)
80	85.04±0.16[a]
160	85.70±0.77[a]
240	86.88±0.80[a]

Values bearing the same small letter superscript(s) do not significantly differ at $p > 0.05$.

Table 2.2 Average degree of polymerization (DP) of debranched (24 h), crystallized (24 h) and filtered products.

Enzyme level (NPUN/g)	DP
80	20.4 ± 0.9^{a}
160	17.8 ± 0.3^{ab}
240	14.6 ± 0.5^{b}

Values bearing the same small letter superscript(s) do not significantly differ at $p > 0.05$.

Table 2.3 Degree of crystallinity (%) of debranched starches at different debranching time. P80, P160 and P240 were samples debranched by 80, 160 and 240 NPUN/g of pullulanase.

Debranching time (h)	Crystallinity (%)		
	P80	P160	P240
1	8.71±0.68[a]	12.83±0.69[a]	9.77±0.13[a]
2	18.42±0.54[b]	21.72±1.38[b]	14.57±1.33[b]
4	20.01±0.68[b]	29.20±0.32[c]	39.26±0.48[c]
8	26.43±0.23[c]	40.82±0.09[d]	57.21±0.90[d]
16	36.65±1.97[d]	50.54±0.19[e]	58.93±0.94[d]
24	45.77±0.81[e]	54.96±1.58[e]	61.91±0.08[e]

Values within columns bearing the same small letter superscript(s) do not significantly differ at $p > 0.05$.

Table 2.4 Rapid digested starch (RDS), slowly digested starch (SDS) and resistant starch (RS) content of starches debranched at 60°C for 24 h, and crystallized at 25°C for 24h and filtered.

Enzyme level (NPUN/g)	RDS (%)	SDS (%)	RS (%)
WMS	34.2±0.6[c]	65.9±0.7[b]	0.0±0[d]
80	23.1±0.6[a]	13.3±0.2[a]	63.6±0.6[a]
160	20.6±0.5[a]	13.2±0.5[a]	66.3±0.1[b]
240	17.3±0.6[b]	12.2±0.1[a]	70.7±0.5[c]

Values within columns bearing the same small letter superscript(s) do not significantly differ at $p > 0.05$.

Table 2.5 Thermal properties of starch debranched by 80 NPUN/g of pullulanase and its enzyme resistant residues during in vitro digestion.

Digestion Time (min)	T_o (°C)	T_p (°C)	T_c (°C)	ΔH (J/g)
0	98.8±0.9^{d}	115.3±0.3^{ab}	139.8±0.3^{b}	18.1±0.2^{a}
20	103.0±0.0^{a}	116.8±0.9^{a}	140.4±0.6^{b}	16.5±0.7^{b}
40	100.2±0.2^{c}	113.7±0.1^{c}	139.8±0.7^{b}	16.7±0.3^{b}
60	102.8±0.1^{a}	114.4±0.1^{bc}	140.2±0.6^{b}	16.5±0.2^{b}
80	100.3±0.7^{c}	116.2±0.2^{a}	143.2±0.7^{a}	17.2±0.6^{ab}
120	102.9±0.0^{a}	115.7±0.0^{ab}	140.3±0.8^{b}	16.6±0.7^{b}
240	101.6±0.1^{b}	115.3±0.1^{ab}	140.0±0.8^{b}	18.1±0.2^{a}

Values within columns bearing the same small letter superscript(s) do not significantly differ at $p > 0.05$.

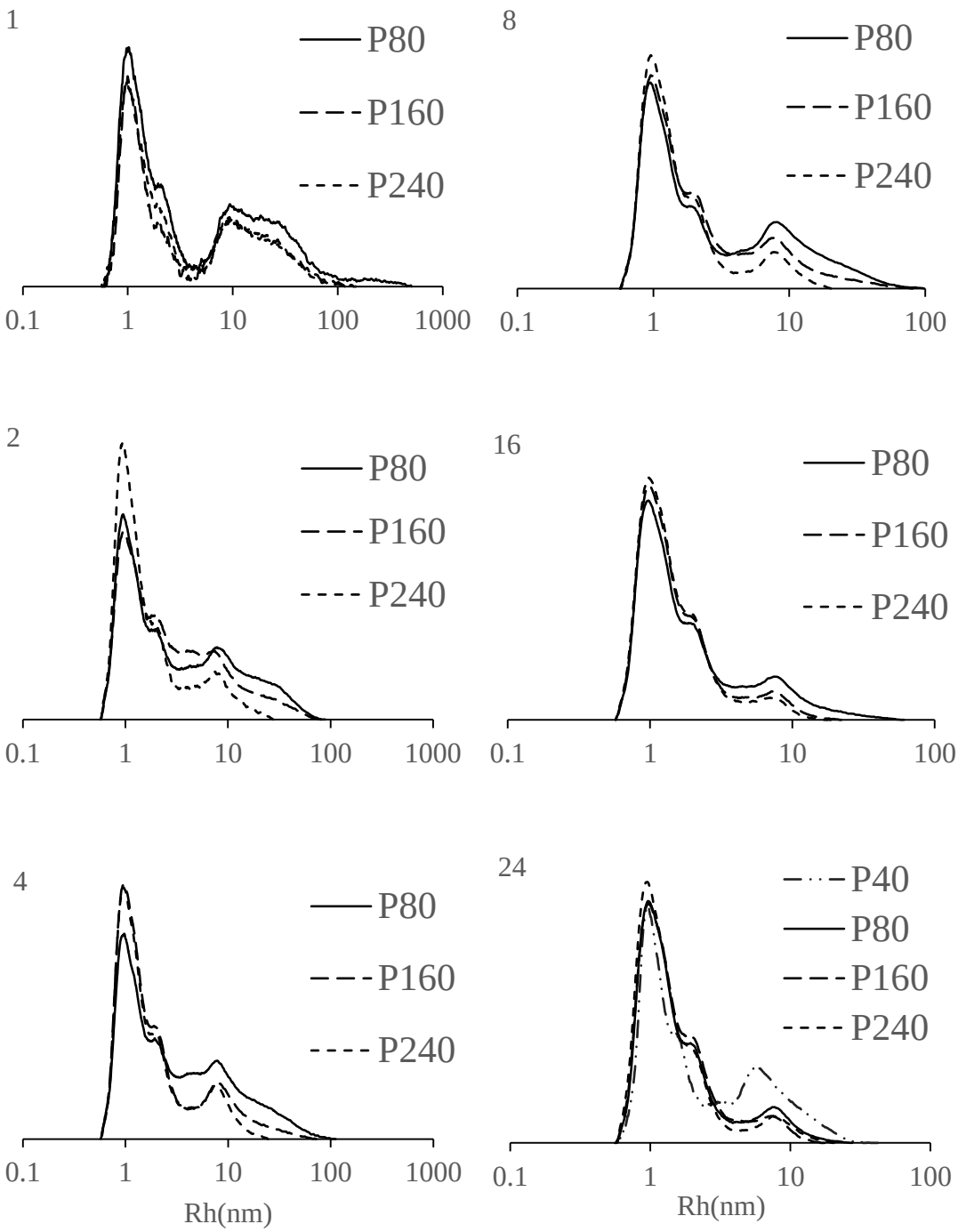

Figure 2.1 Molecular size distribution of debranched waxy maize starches. 1, 2, 4, 8, 16 and 24 indicate that the debranching times (h) respectively. P40, P80, P160, and P240 indicate that the sample was treated by 40, 80, 160 and 240 NPUN/g of pullulanase, respectively.

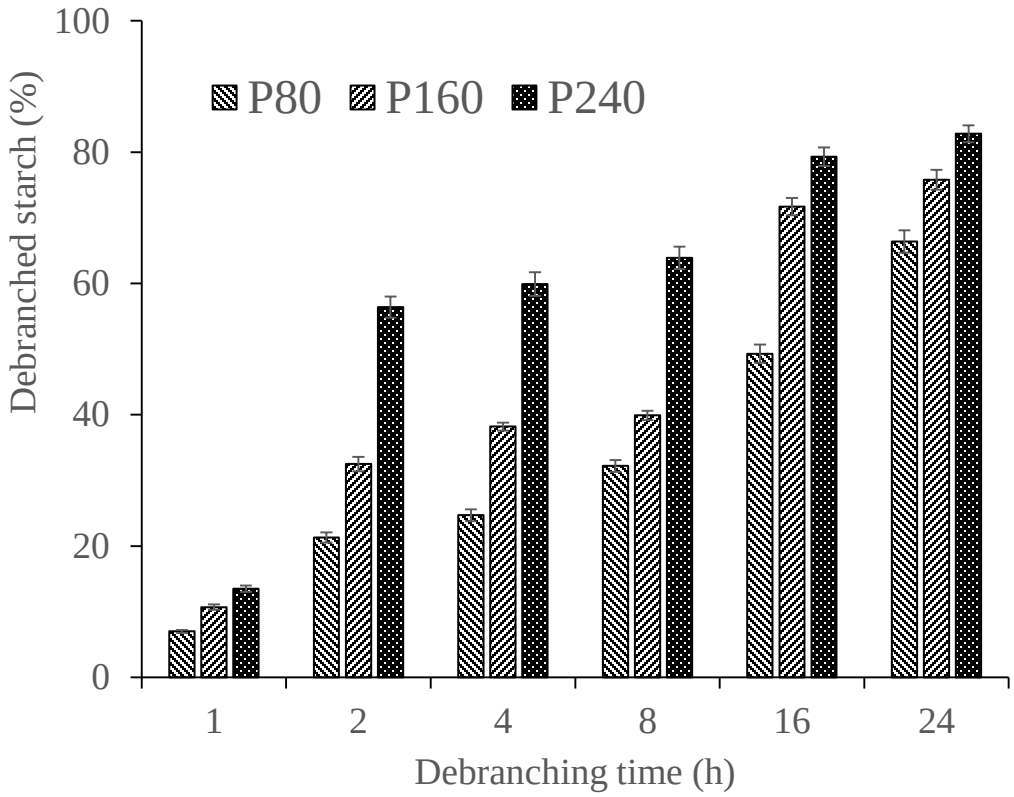

Figure 2.2 The debranching degree (%) at different debranching times.

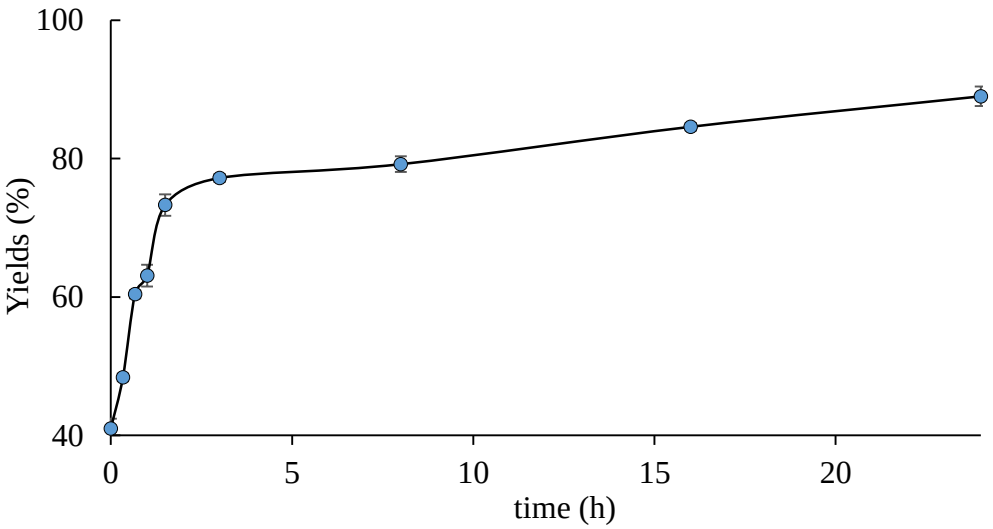

Figure 2.3 Yields of debranched starches crystallized at 25°C and 25% solids after debranching at 60°C for 24 h. Starches were debranched by 80 NPUN/g of pullulanase. Same yield was obtained when 160 and 240 NPUN/g of pullulanase were used.

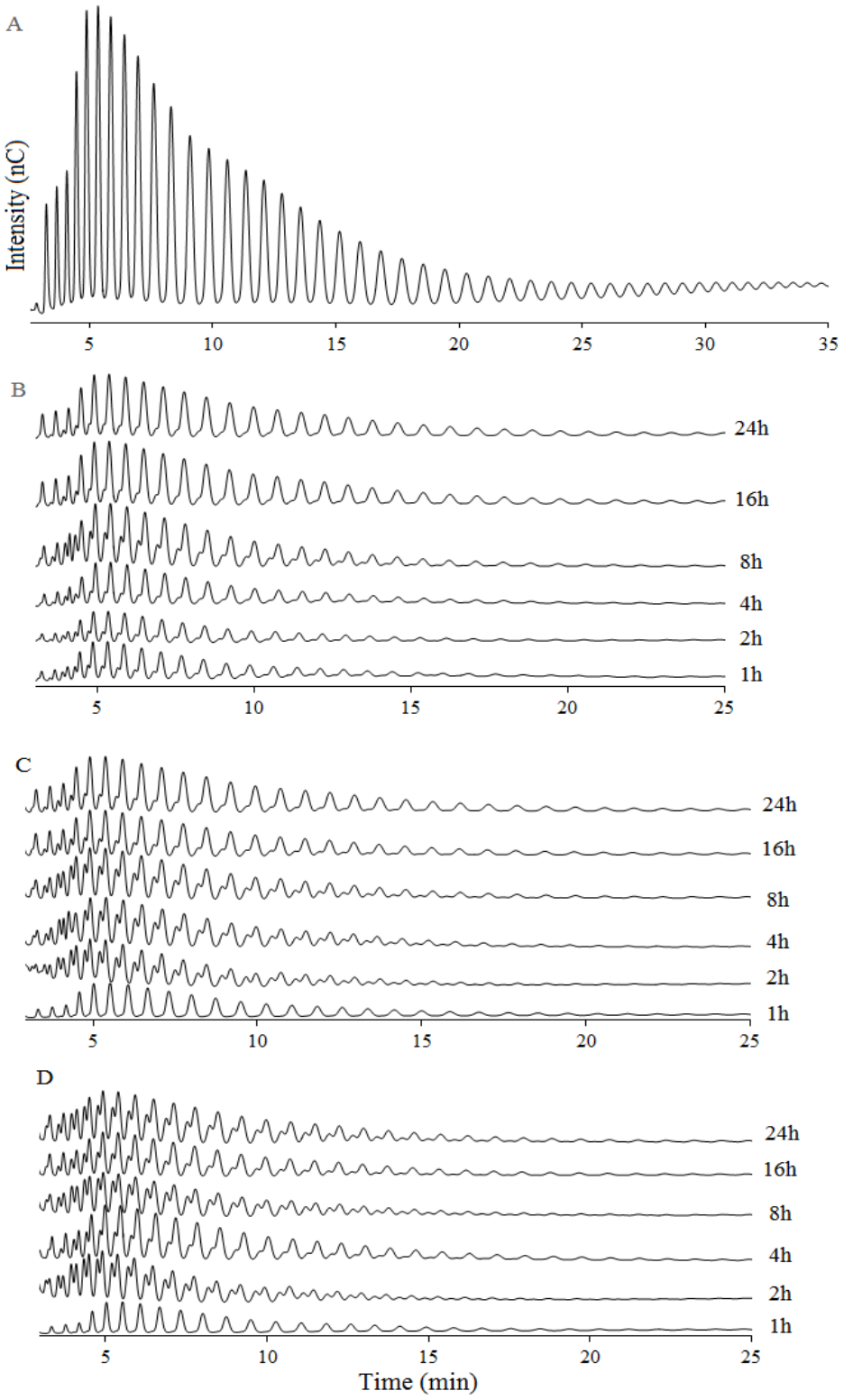

Figure 2.4 Chromatograms of waxy maize starch debranched by isoamylase (A), and 80 (B), 160 (C), and 240 (D) NPUN/g of pullulanase as determined by HPAEC.

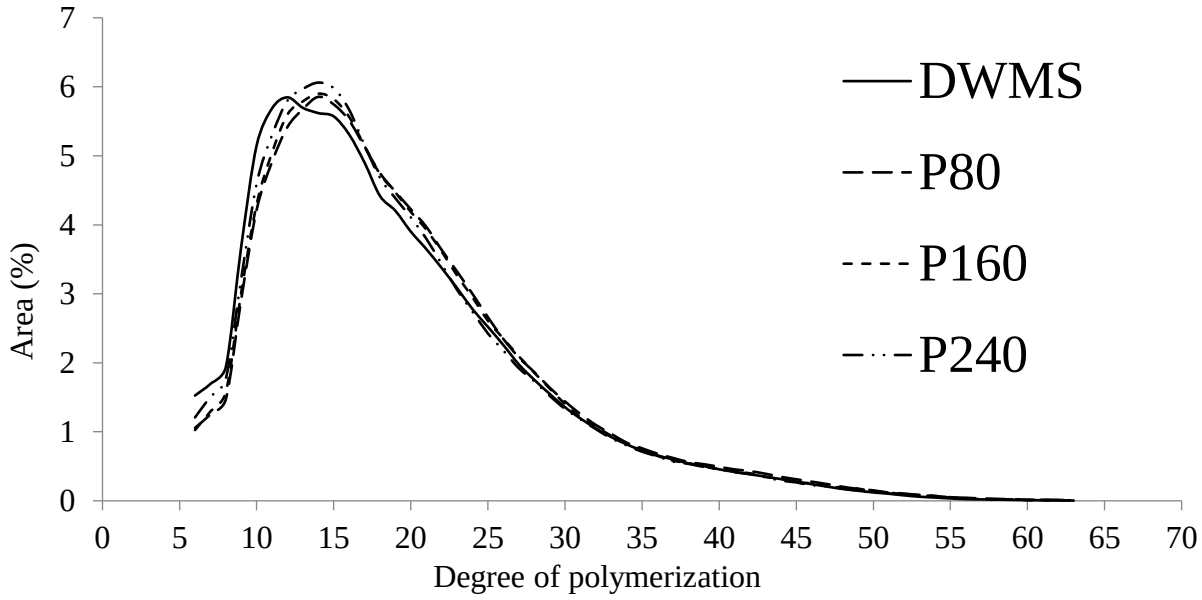

Figure 2.5 Chain length distribution of waxy maize starch debranched by isoamylase (DWMS), and 80 (P80), 160 (P160), and 240 (P240) NPUN/g of pullulanase as determined by HPAEC.

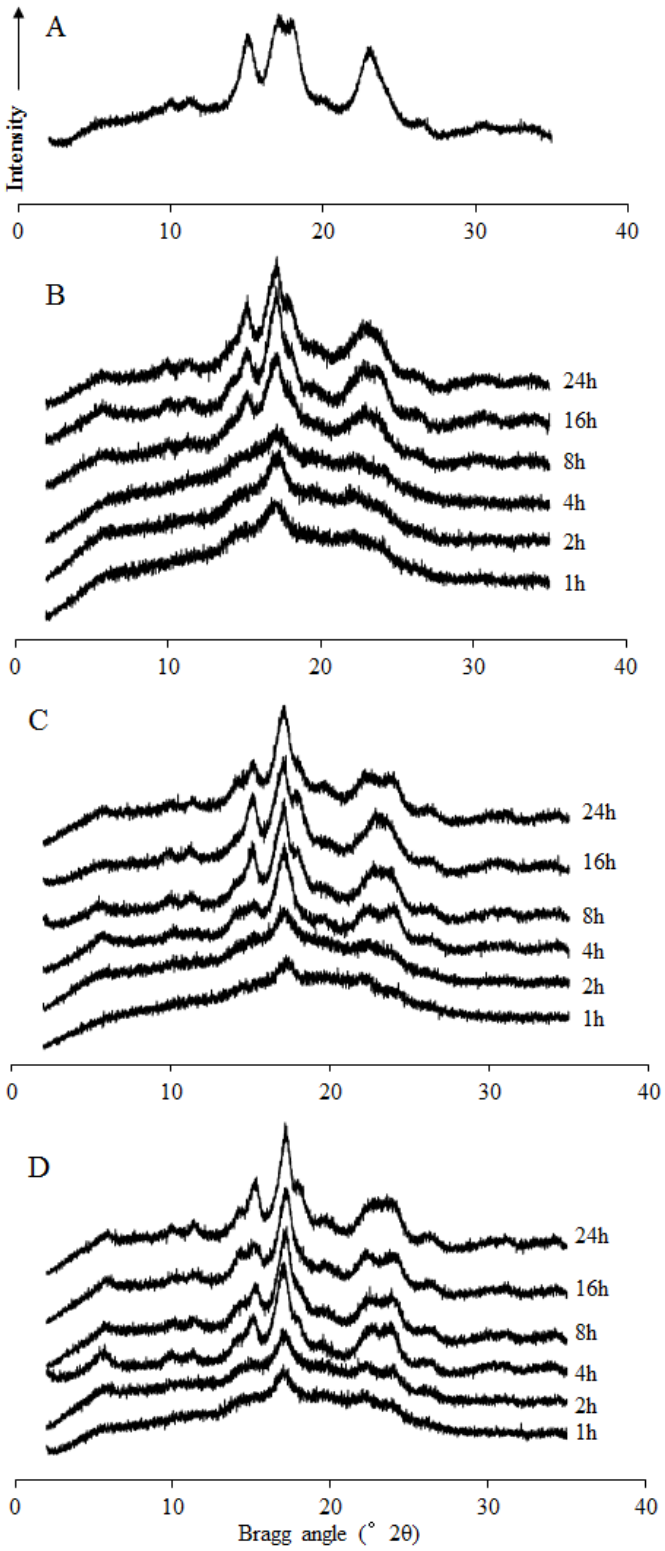

Figure 2.6 X-ray diffraction of waxy maize starch (A) and debranched waxy maize starch treated by 80 NPUN/g (B), 160 NPUN/g (C) and 240 NPUN/g (D) of pullulanase.

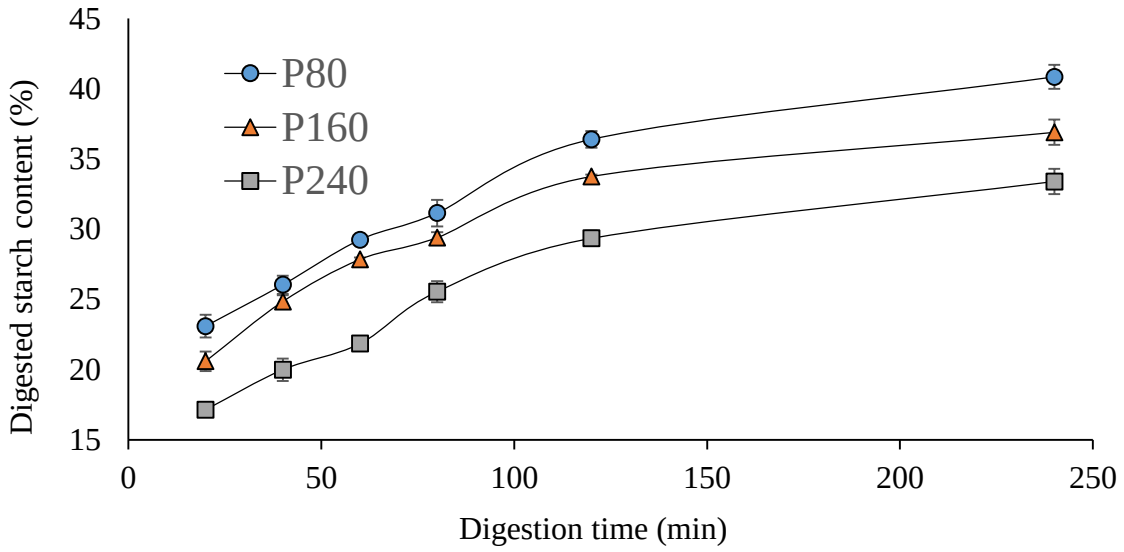

Figure 2.7 Digestion curves of debranched, crystallized and filtered starches. P80, P160 and P240 were debranched by 80, 160 and 240 NPUN/g of pullulanase, respectively.

Chapter 3 - Structure and digestibility of spherulites produced from debranched waxy maize starches

Introduction

After starch is gelatinized, during cooling and storage, crystallization normally results in A-type or B-type crystalline structure, depending on degree of polymerization (DP) of starch and crystallization conditions such as temperature, starch concentration, and solvent used (Jane, 2004). High solids concentrations, high temperatures and shorter chains tend to result in A-type crystalline products (Gidley & Bulpin, 1987; Pohu et al., 2004). B-type crystals were produced when 25% debranched waxy maize starches were crystallized at 4 and 25°C, whereas A-type crystallites were observed when crystallized at 50°C (Cai & Shi, 2014). On the other hand, B-type crystals were produced at 50°C when the solids concentration was 5%, or 25% when the parent starch was waxy potato, which had a longer chain length than waxy maize (Cai & Shi, 2010, 2014). In addition, A-type crystal formation from amylodextrins can be enhanced by the addition of ethanol (Helbert et al., 1993; Ring et al., 1987) or salt (Hizukuri et al., 1960).

Spherulites are crystalline materials with a notably spherical form, requiring some measure of rotational symmetry, and generally displaying a Maltese cross (Haudin, 1986). The formation of starch spherulites has been described as “high temperature retrogradation” and involves the recrystallization of fully dissolved starches under controlled conditions (Fanta, et al., 2002). Starch based spherulites can be formed by heating and cooling a starch slurry. The

heating temperature needs to be very high, over 140°C to fully dissolve the starch (Singh et al., 2010). When normal corn starch was used to produce spherulites, spherocrystals were observed at slow cooling rates (Fanta et al., 2002) and rapid cooling rate with the addition of 1-hexadecylamine (Fanta, et al., 2013) or fatty acid (Fanta, et al., 2008). In the work by Fanta et al. (2013), there is evidence indicating rapid cooling produces smaller spherulites whose morphology is mostly influenced by the hydrophobic structure. Differential scanning calorimetry (DSC) has been used to prepare spherulites and samples were heated to 180°C (Creek et al., 2006). DSC has the benefit of being able to control temperature and cooling rates accurately, and can be used to produce spherulites with different starches, solid concentrations and heating temperatures (Ziegler, et al., 2003).

Microwave and jet cooking have been used for producing larger quantities (Felker, et al., 2013). Jet cooking produced uniform, large, toroidal spherulites; however, microwave processing yielded smaller disc-shaped spherulites. The mechanical shear of jet cooking was thought to overcome the limits of amylose solubility, and enhance the formation of spherulites.

Spherulites can be produced using starches containing significant amounts of amylose; and indeed, higher amylose starch more readily forms spherulites when compared to normal and waxy starches (Nordmark & Ziegler, 2002c; Singh et al., 2010). With more linear molecules, the formation of spherulites is easier, but for high-amylose starch or native starch, the molecular weight (MW) range is relatively large, which inhibits the formation of products with higher degree of crystallinity; whereas debranching waxy starch can form linear molecules with a

relatively narrow size range (Shi et al., 2006). Cai & Shi (2014) produced spherulites with debranched waxy maize starches and debranched waxy potato starches. Cooked debranched starches were re-crystallized at 25°C, and spherulites derived from debranched waxy potato starches had lower resistance to enzyme digestion. Debranched waxy potato starches had larger average chain length and are also phosphorylated, which may affect the organization of spherulites, and result in different resistant starch contents.

The primary technique for checking the quality of the formation of spherulites is light microscopy. Using crossed polarizers, the addition of a full-wave red retardation plate provides the advantage of differentiating regions of additive and subtractive interference, thereby highlighting and clarifying the orientation of crystals in the overall structure (Kiatponglarp et al., 2016; Kobayashi et al., 2000). The birefringence sign of polymer spherulites are can be conventionally classified as positive or negative using the standard equation $\Delta n = n_1 - n_2$, where n_1 is the arbitrarily the optical axis radiating from the center of the spherulites, and n_2 is perpendicular to n_1. This method of classification is widely used in spherulites for a long time (Haudin, 1986). Native starch granules from any natural species serve as a reference and are definitive of the positive structure, which for our apparatus and figures are seen with the blue (subtractive) quadrants occupying the North-East and South-West quadrants, whereas where the yellow (additive) regions occur there instead, we define those structures as negative (Kobayashi et al., 2000). As a general rule, positive spherulites indicate the orientation of helices is radial, and the negative pattern means the orientation is concentric, and usually toroid (Haudin, 1986).

In previous work, spherulites have been produced with debranched waxy maize starch after hydrolysis by isoamylase (Cai & Shi, 2013), but the internal structure of spherulites was not thoroughly investigated. The objective of this study was to develop the means to control crystallization of debranched starch, so that spherulites with different types of crystal, different internal organizations, and digestibility could be produced.

Materials and Methods

Materials

Waxy maize (Amioca) starch was obtained from Ingredion Inc. (Bridgewater, NJ). Pullulanase (Promozyme D6, 4000 NPUN/g) was obtained from Novozyme (Franklinton, NC). One pullulanase unit (NPUN) is defined as the amount of enzyme, which, under standard conditions (pH=5, 40°C, incubation of 20 min), hydrolyzes pullulan, liberating reducing carbohydrate with reducing power equivalent to 1 μmole glucose per minute. Other chemicals were analytical grade.

Debranching starch

Waxy maize starch (100g, db) was mixed with 300 g de-ionized water in a pressure bottle (1L, ACE glass, Vineland, USA). The mixture was adjusted to pH using 6, stirred with a magnetic stirring bar and heated in a boiling water bath for 30 minutes. The mixture was then heated in an oven at 120°C for 30 minutes. After the mixture was cooled to 60°C, pullulanase (2% db) was added and the mixture was incubated in a water bath at 60°C for 24 hours with

constant shaking. After that, the mixture was placed at 25°C for 24 hours, the yields of crystallite at different time points were determined by centrifuging the mixture and measuring the soluble carbohydrate content with a portable refractometer (Fisher Scientific Inc., Pittsburgh, PA, USA). The slurry was filtered and the cake was dried in an oven at 40°C overnight (Cai, Shi, Rong, & Hsiao, 2010; Cai & Shi, 2010).

Spherulites formation

Suspensions of 5 g of debranched starch in 15 g water were prepared in 4 cm diameter aluminum RVA cans (Perten Instruments. Hägersten, Sweden). Two cans containing the mixture were loaded in a pressure reactor (4521M, PARR, Illinois, USA) and heated to 183°C. The pressure reactor was then cooled with running tap water flowing through internal cooling pipes. When the temperature dropped to 115.5°C, the pressure in the reactor was released, and the samples were taken out when temperature dropped to 90°C.

Four crystallization conditions were studied and compared: 1) Samples were placed in a refrigerator and held at 4°C for 24 hours; 2) Ethanol (equal volume to water) was added into samples gently without mixing before being placed into the refrigerator and held at 4°C for 24 hours. (Helbert et al., 1993); 3) Samples were moved to a 50°C water bath and held at 50°C for 24 hours; and 4) Samples were moved to a 50°C water bath and held at 50°C for 24 hours and then placed in a refrigerator (4°C) for another 24 hours.

In this study, samples crystallized at 4°C by adding ethanol are referred to as “ES4”; while those crystallized in water at 4°C are “WS4”. “WS50” products are spherulites crystallized in water at 50°C and collected without cooling, and “WS50-4” are spherulites crystallized at 50°C first and then further crystallized at 4°C. During the crystallization, any disturbance to the samples was avoided as movement of the fluid may inhibit the formation of spherulites.

All crystallized samples were vacuum filtered and dried in an oven at 40°C for 12 hours. The weight of each dried sample was measured to calculate yield.

Light microscopy

Samples were dispersed in 50% glycerol solution (1%, w/v), and a drop was deposited on a microscope slide with a coverslip. The sample was observed by an Olympus BX51TF microscope attached with a retardation plate (Olympus Optical Co. Ltd., Shinjuku-ku, Tokyo, Japan). Samples were observed in normal, cross-polarized light, and cross-polarised light with full-wave red retardation, and the images were captured by a SPOT 18.2 Color Mosaic camera (Diagnostic Instruments Inc., Sterling Heights, MI, USA).

GPC

From each sample, 4 mg of solid was dissolved in 4 ml of dimethyl sulfoxide (DMSO) (HPLC grade) containing lithium bromide (0.5% w/w) (Vilaplana & Gilbert, 2010). The mixture was tightly sealed and stirred in a boiling water bath for 24 hours, cooled to 25°C, filtered through a 0.45 µm filter and then injected into a PL-GPC 220 instrument (Polymer Laboratories,

Inc., Amherst, MA, USA) equipped with three Phenogel columns (Cai et al., 2010) (Phenomenex, Inc., Torrance, CA, USA) and a guard column (Phenomenex, Inc., Torrance, CA, USA). The eluent was DMSO containing 0.5% (w/w) LiBr, and the flow rate was 0.8 mL/min. Temperature was controlled at 80°C. Pullulan standards were used for universal calibration (Vilaplana & Gilbert, 2010).

High-performance anion exchange chromatography (HPAEC)

Chain length distribution (CLD) was determined by HPAEC (Dionex ICS-3000, Dionex Corp., Sunnyvate, CA, USA), equipped with a pulsed amperometric detector, a guard column, a CarboPacTM PA1 analytical column and an AS-DV autosampler. Starch (5 mg) was dissolved in 5 ml of water in a boiling water bath for 1 h with stirring. The eluents were prepared as described previously (Shi & Seib, 1992). Eluent A was 150 mM NaOH, and eluent B was 150 mM NaOH containing 500 mM sodium acetate. The gradient program used eluent B in the proportions: 40, 50, 60, and 80% at 0, 2, 10, and 40 min, respectively. The separations were carried out at 25°C and the flow rate was 1 ml/min. Maltohexaose (DP=6) was used as standard.

X-ray diffraction (XRD)

The moisture of samples was adjusted to about 17% using a saturated sodium chloride solution in a humidity chamber. The crystalline structure of debranched starch was determined by wide-angle X-ray diffraction (PANalytical, Almelo, The Netherlands). The measurements were conducted at 35 kV and 20 mA, theta-compensating slit, and a diffracted beam

monochromator. The diffractograms were recorded between 2 and 35° (2θ). Relative degree of crystallinity was calculated by the ratio of the peaks representing crystals to the total area (Komiya & Nara, 1986).

Digestibility of spherulites

A modified Englyst method was used (Englyst et al., 1992; Sang & Seib, 2006). Samples were digested by pancreatin and amyloglucosidase, then 4 ml of digested sample solution was transferred into 20 ml of ethanol after 20, 40, 60, 80, 120 and 240 min.

Statistical analysis

The analyses of variance (ANOVA) mean values were determined by Minitab 17 Statistical Software Program (Minitab Inc. State College PA, USA). Mean value and standard deviation from the duplicated experiments were reported.

Results and Discussion

Molecular size distribution and yields

Samples crystallized at 4°C had similar molecular size distributions, but WS50 had a relatively narrow size range and contained less large molecules (Figure 3.1). At 50°C, large branched molecules were probably disproportionately lost by filtration as they were not crystalized; but with further crystallization at 4°C, these molecules also formed crystals, resulting in the same molecular size distribution for all the samples crystallized at 4°C.

The yield of crystallites was 82 to 87% when crystallized at 4°C (Table 3.1). However, if the product was crystallized at 50°C, the yield was much lower, and was about 45%. This result was matched with the work by Cai and Shi (2013). When a sample was crystallized at 50°C, large molecules (Rh>13 nm) were not crystallized, so the yields was low. But when sample WS50 was further crystallized at 4°C, the yields was increased due to large molecules were crystallized.

Chain length distribution

In the four crystallized samples, few molecules were larger than DP 60 and most molecules were smaller than DP 30 (Figure 3.2). For all samples, a peak was detected around DP 15 Samples ES4 and WS50 had a greater proportion of molecules with unit chains between DP 11 to 18 than samples WS4 and WS50-4 (Figure 3.2). ES4 contained more molecules of DP 6-19, which was about 67.1%. WS50 contained less molecules of DP 6-19 (about 64.3%). WS4 and WS50-4 had similar chain length distribution, and the molecules of DP 6-19 were about 61% (Table 3.2).

After ethanol was added, the starch molecules contacted with ethanol were precipitated immediately, so the proportion of molecules between DP 6 to 19 was relatively higher in ES4 than in the other samples (Figure 3.2). According to Eerlingen (1993), the DP of resistant starch (RS) was higher than 19, and the RS content was increased with higher DP (up to 100) of amylose (Eerlingen et al. 1993). So, the table 3.2 agreed to the results of digestibility. Based on

the results of GPC (Figure 3.1), when debranched waxy maize starches were crystallized at 50°C in water, larger molecules were not precipitated, a result also reflected by HPAEC (Figure 3.2).

X-ray diffraction (XRD)

Spherulites formed in water and ethanol at 4°C (WS4 and ES4) displayed a B-type X-ray diffraction pattern, whereas spherulites formed at 50°C (WS50) showed an A-type pattern. When spherulites formed at 50°C and further cooled to 4°C (WS50-4), the pattern was still an A-type with a slightly weaker peak at 12 °2θ (Figure 3.3). When spherulites were formed at 4°C (WS4 and ES4), the degree of crystallinity was close (about 58.0%). When debranched starch was crystallized at 50°C (WS50), the degree of crystallinity was increased to 66.6%. With cooling from 50 to 4°C, more molecules were crystallized and the degree of crystallinity was increased to 76.0% (Table 3.3).

The type of starch crystalline structure is influenced by degree of polymerization of the starting material. There is evidence that when crystallized at 25°C, A-type crystals develop for DP 10-12 and B-type for DP 13 and above (Gidley & Bulpin, 1987b). Further evidence shows that the molar percent of the DP 10-13 molecules is influential on crystalline types (Cheetham & Tao, 1998). B-type spherulites has been produced with debranched waxy maize starch crystallized at 4°C and A-type crystalline product by crystallization at 50°C (Cai & Shi, 2013). It has also been reported that A-type spherulites can be obtained by adding ethanol (30% w/w) prior to crystallization (Ring et al., 1987). A-type spherulites were formed by adding a volume of

ethanol equal to that of the aqueous solution slowly, when the aqueous solution was reduced to 78°C (Helbert et al., 1993). However, ES4 displayed a B-type refraction pattern in this study. Ethanol was added gently when the starch solution was reduced to 90°C. This ethanol layer was initially in a separate phase on the top of the starch solution. The starches on the top surface were precipitated immediately. Starches at the interface were crystallized by ethanol, but the starches within the aqueous solution hardly came into contact with the ethanol. As a result, most of the spherulites produced showed a B-type diffraction pattern. When the sample was stirred after adding ethanol, A-type crystalline pattern was produced since the precipitation was more influenced by ethanol. But the crystalline product showed no Maltese cross in this case. When starches were further crystallized at 4°C, B-type crystallinity might have been formed by the large molecules, but the amount of B-type material was too small to be observed.

Morphology of spherulites

Native starches were used as standards to define positive birefringence and orientate the images to contain a "+" shaped Maltese cross (Figure 3.4, WMS). ES4 had positive Maltese crosses (Figure 3.4, ES4), and the size of spherulites was about 10 μm. The images of WS4 (Figure 3.4, WS4) and WS50 (Figure 3.4, WS50) were similar to those of Cai & Shi (2013). WS4 was smaller than ES4, and was about 8 μm. However, the orientation of cross-like patterns in WS4 was neither positive nor negative, but a cross rotated around 45° from the positive orientation. This indicates that the structure of particle was neither radial nor concentric, but

likely had parallel crystals that spiraled outwards from the center in a broad toroid. Compared to WS4 and ES4, WS50 was much smaller and no clear Maltese cross was observed. Under red-retarded light, particles demonstrated pure blue or yellow, which indicates that the structure was organized in a unidirectional parallel fashion. With further crystallization at 4°C, positive birefringence was observed for same particles, although many particles were still pure blue or yellow (Figure 3.4, WS50-4). It is possible that the crystallites formed at 50°C played a role as a core during the crystallization at 4°C, so that the size of particles increased (10 ~ 20 μm) and the surface became less smooth. Some molecules, which were not crystallized at 50°C, were crystallized and formed spherulites at 4°C.

Digestibility of spherulites

Spherulites formed in ethanol (ES4) was more digestible than the other three samples. ES4 and WS50 were digested faster in the first 2 hours, whereas the digestion curves of WS4 and WS50-4 were more linear. Compared to ES4, WS4 was less digested after two hours, but had similar digestion pattern after 4 hours. The digestion rate of WS50-4 was the slowest, and its digested starch content was the lowest after 20 min (Figure 3.5). When samples were crystallized at 4°C, adding ethanol (ES4) resulted in lower RS content (52.6%). When samples were crystallized in water at 4°C (WS4), the RS content was 62.8%. When the crystallization temperature increased to 50°C (WS50), the RS content decreased to 60%. If the samples were

crystallized at 50°C for 24 hours and then crystallized 4°C for another 24 hours (WS50-4), the RS content was the highest (73.0%) (Table 3.4).

Evans & Thompson (2008) also observed that starch precipitated by ethanol had lower RS content. RS content may be influenced by the composition of different starches. Debranched starches crystallized at 50°C had the highest RS content and the crystallites showed an A-type diffraction pattern (Cai & Shi, 2013, 2014). Compared to B-type crystallites, A-type crystallites have a dense structure and fewer water molecules in the monoclinic unit cell. As a result, after crystallization of the same linear material, A-type crystallites have a greater resistance than B-type to enzyme digestion. In Cai and Shi's work (2013), the RS content of sample crystallized at 50°C was higher than 90%, and other spherulites formed in water showed high RS content (more than 80%). In that study (Cai & Shi, 2013), the starch used to produce spherulites contained no branched molecules. Although the RS content of WS50 in this study was 60%, the RS content was increased by 13% when it was further crystallized at 4°C, which resulted in higher degree of crystallinity (Table 3.3).

At the beginning of enzyme digestion, the macrocrystalline structure of WS4 was quickly degraded into smaller fragments (Figure 3.7 A, B). Although fragments were produced in ES4, positive birefringence was still observed, indicating their structural integrity was maintained (Figure 3.6 A, B), and some spherulites were robust enough to keep the ordered macrocrystalline structure. After longer digestion times, the proportion of large particles was actually increased in 90 min and then decreased again (Figure 3.6 C, D, E, F; Figure 3.7 C, D, E, F). Once the smallest

particles were largely removed, larger particles were fragmented, resulting again in more small particles.

Sample WS50 contained small particles and displayed no Maltese crosses (Figure 3.8). As a result, changes in morphology during digestion were subtler than that of the other samples (Figure 3.8). Large, round particles with positive birefringence were observed in the beginning digestion of WS50-4 and then disintegrated into small fragments (Figure 3.9).

Thermal properties

When samples were crystallized at 4°C in water (WS4), the enthalpy (ΔH) was 25.6 J/g. With adding ethanol, the ΔH was 22.4 J/g; T_o was decreased from 59.8 to 56.4°C. When sample was crystallized in water at 50°C (WS50), T_o (67.4°C) and ΔH (33.4J/g) were higher. With further cooling to 4°C (WS50-4), ΔH was increased to 47.2 J/g, but T_o of WS50-4 was 62.8°C (Table 3.5).

In this study, WS4 and ES4 showed B-type pattern (Figure 3.3) and lower melting temperature (Table 3.5). The comparison of melting temperature between A-type and B-type crystalline starch have been reported (Cai & Shi, 2013; Whittam et al., 1990). In Cai and Shi's work, linear starch molecules were crystallized at 4°C and 50°C, showing B-type and A-type pattern, respectively. In this study, WS4 and ES4 showed B-type pattern and had lower melting temperatures. The end melting temperature of A-type crystalline was about 30°C higher than that of B-type crystalline. According to Lopez-Rubio et al. (2008), enthalpy value was influenced by

the degree of crystallinity. As a result, the enthalpy was increased when the degree of crystallinity was higher (Table 3.3 and Table 3.5).

Conclusions

Debranched waxy maize starch crystallized in water at 4°C produced spherulites of neither positive nor truly negative birefringence, whereas positive birefringence resulted from the addition of ethanol. Both spherulites crystallized at 4°C were B-type crystalline structure. When debranched starches were crystallized at 50°C, no Maltese cross was observed and the particles were smaller; but with further crystallization at 4°C, positive birefringence developed in some particles, and the bulk of the crystallites maintained A-type crystallinity. When ethanol was introduced, RS content was the lowest (52.6%). RS contents in those samples crystallized in water at 4 and 50°C were 62.8% and 60.0%, respectively. By further crystallization of WS50 at 4°C, WS50-4 contained more RS (73.0%) and also showed the highest degree of crystallinity (76%) and enthalpy (47.2 J/g). The signs of birefringence were determined after observing under full-wave red retardation, but the internal structure of crystallites merits further study. Further experiments may lead to crystallites of greater RS content, and may also facilitate a greater understanding of starch crystallization.

Reference

Cai, L., & Shi, Y.-C. (2010). Structure and digestibility of crystalline short-chain amylose from debranched waxy wheat, waxy maize, and waxy potato starches. *Carbohydrate Polymers*, *79*, 1117–1123.

Cai, L., & Shi, Y.-C. (2013). Self-assembly of short linear chains to A- and B‑type starch spherulites and their enzymatic digestibility. *Journal of Agricultural and Food Chemistry*, *61*, 10787−10797.

Cai, L., & Shi, Y.-C. (2014). Preparation, structure, and digestibility of crystalline A- and B-type aggregates from debranched waxy starches. *Carbohydrate Polymers*, *105*, 341–350.

Cai, L., Shi, Y.-C., Rong, L., & Hsiao, B. S. (2010). Debranching and crystallization of waxy maize starch in relation to enzyme digestibility. *Carbohydrate Polymers*, *81*, 385–393.

Cheetham, N. W., & Tao, L. (1998). Variation in crystalline type with amylose content in maize starch granules: an X-ray powder diffraction study. *Carbohydrate Polymers*, *36*, 277–284.

Creek, J. A., Ziegler, G. R., & Runt, J. (2006). Amylose crystallization from concentrated aqueous solution. *Biomacromolecules*, *7*, 761–770.

Eerlingen, R. C., Deceuninck, M., & Delcour, J. A. (1993). Enzyme-resistant starch. II. Influence of amylose chain length on resistant starch formation. *Cereal Chemistry*, *70*, 345–350.

Englyst, H. N., Kingman, S. M., & Cummings, J. H. (1992). Englyst et al Classification and measurement of nutritionally important starch fractions. *European Journal of Clinical Nutrition*, *46*, S33–S50.

Evans, A., & Thompson, D. B. (2008). Enzyme susceptibility of high-amylose starch precipitated from sodium hydroxide dispersions. *Cereal Chemistry*, *85*, 480–487.

Fanta, G. F., Felker, F. C., & Shogren, R. L. (2002). Formation of crystalline aggregates in slowly-cooled starch solutions prepared by steam jet cooking. *Carbohydrate Polymers*, *48*, 161–170.

Fanta, G. F., Felker, F. C., Shogren, R. L., & Salch, J. H. (2008). Preparation of spherulites from jet cooked mixtures of high amylose starch and fatty acids. Effect of preparative conditions on spherulite morphology and yield. *Carbohydrate Polymers*, *71*, 253–262.

Fanta, G. F., Kenar, J. A., & Felker, F. C. (2013). Preparation and properties of amylose complexes prepared from hexadecylamine and its hydrochloride salt. *Carbohydrate Polymers*, *98*, 555–561.

Felker, F. C., Kenar, J. A., Fanta, G. F., & Biswas, A. (2013). Comparison of microwave processing and excess steam jet cooking for spherulite production from amylose-fatty acid inclusion complexes. *Starch - Stärke*, *65*, 864–874.

Gidley, M. J., & Bulpin, P. V. (1987). Crystallisation of malto-oligosaccharides as models of the crystalline forms of starch: minimum chain-length requirement for the formation of double helices. *Carbohydrate Research*, *161*, 291–300.

Haudin, J. M. (1986). Optical studies of polymer morphology. In *optical properties of polymers* (pp. 167–264). London: Elsevier Applied Science Publishers.

Helbert, W., Chanzy, H., Planchot, V., Buléon, A., & Colonna, P. (1993). Morphological and structural features of amylose spherocrystals of A-type. *Int. J. Biol. Macromol.*, *15*, 183–187.

Hizukuri, S., Fujii, M., & Nikuni, Z. (1960). The effect of inorganic ions on the crystallization of amylodextrin. *Biochimica et Biophysica Acta*, *40*, 346–348.

Jane, J. (2004). Starch: Structure and Properties. In *Chemical and Functional Properties of Food Saccharides* (pp. 81–100). 2000 N.W. Corporate Blvd., Boca Raton, Florida: CRC Press.

Kiatponglarp, W., Rugmai, S., Rolland-Sabaté, A., Buléon, A., & Tongta, S. (2016). Spherulitic self-assembly of debranched starch from aqueous solution and its effect on enzyme digestibility. *Food Hydrocolloids*, *55*, 235–243.

Kiatponglarp, W., Tongta, S., Rolland-Sabaté, A., & Buléon, A. (2015). Crystallization and chain reorganization of debranched rice starches in relation to resistant starch formation. *Carbohydrate Polymers*, *122*, 108–114.

Kobayashi, S., Hobson, L. J., Sakamoto, J., Kimura, S., Sugiyama, J., Imai, T., & Itoh, T. (2000). Formation and structure of artificial cellulose spherulites via enzymatic polymerization. *Biomacromolecules*, *1*, 168–173.

Komiya, T., & Nara, S. (1986). Changes in crystallinity and gelatinization phenomena of potato starch by acid treatment. *Starch - Stärke*, *38*, 9–13.

Lopez-Rubio, A., Flanagan, B. M., Gilbert, E. P., & Gidley, M. J. (2008). A novel approach for calculating starch crystallinity and its correlation with double helix content: A combined XRD and NMR study. *Biopolymers*, *89*, 761–768.

Nordmark, T. S., & Ziegler, G. R. (2002). Spherulitic crystallization of gelatinized maize starch and its fractions. *Carbohydrate Polymers*, *49*, 439–448.

Pohu, A., Planchot, V., Putaux, J. L., Colonna, P., & Buléon, A. (2004). Split crystallization during debranching of maltodextrins at high concentration by isoamylase. *Biomacromolecules*, *5*, 1792–1798.

Ring, S. G., Miles, M. J., Morris, V. J., & Turner, R. (1987). Spherulitic crystallization of short chain amylose. *Int. J. Biol. Macromol.*, *9*, 158–160.

Sang, Y., & Seib, P. A. (2006). Resistant starches from amylose mutants of corn by simultaneous heat-moisture treatment and phosphorylation. *Carbohydrate Polymers*, *63*, 167–175.

Shi, Y.-C., Cui, X., Birkett, A. M., & Thatcher, M. G. (2006). Resistant starch prepared by isoamylase debranching of low amylose starch. Pat. No. 7 081 261.

Shi, Y.-C., & Seib, P. A. (1992). The structure of four waxy starches related to gelatinization and retrogradation. *Carbohydrate Research*, 227, 131–145.

Singh, J., Lelane, C., Stewart, R. B., & Singh, H. (2010). Formation of starch spherulites: Role of amylose content and thermal events. *Food Chemistry*, *121*, 980–989.

Vilaplana, F., & Gilbert, R. G. (2010). Two-dimensional size/branch length distributions of a branched polymer. *Macromolecules*, *43*, 7321–7329.

Whittam, M. ., Noel, T. R., & Ring, S. G. (1990). Melting behaviour of A- and B-type crystalline starch. *International Journal of Biological Macromolecules*, *12*, 359–362.

Ziegler, G. R., Nordmark, T. S., & Woodling, S. E. (2003). Spherulitic crystallization of starch: influence of botanical origin and extent of thermal treatment. Food Hydrocolloids, 17, 487–494.

Table 3.1 Yields of spherulites formed in ethanol at 4°C (ES4), in water at 4°C (WS4), in water at 50°C (WS50) and in water from 50°C to 4°C (WS50-4).

Spherulites	Yields (%)
ES4	82.07 ± 0.79^{b}
WS4	82.20 ± 0.37^{b}
WS50	44.51 ± 0.51^{c}
WS50-4	86.48 ± 0.07^{a}

Values within columns bearing the same small letter superscript(s) do not significantly differ at $p > 0.05$.

Table 3.2 Percentage of molecules from DP 6 to 19 in samples formed in ethanol at 4°C (ES4), in water at 4°C (WS4), in water at 50°C (WS50) and in water from 50°C to 4°C (WS50-4), respectively.

Sample	ES4	WS4	WS50	WS50-4
DP 6-19 (%)	67.1 ± 0.9^{a}	61.3 ± 0.6^{b}	64.3 ± 0.7^{ab}	61.0 ± 0.3^{b}

Values within columns bearing the same small letter superscript(s) do not significantly differ at $p > 0.05$.

Table 3.3 Degree of crystallinity (%) of samples formed in ethanol at 4°C (ES4), in water at 4°C (WS4), in water at 50°C (WS50) and in water from 50°C to 4°C (WS50-4), respectively.

Sample	ES4	WS4	WS50	WS50-4
Crystallinity (%)	58.4 ± 0.4^{b}	58.0 ± 0.6^{b}	66.6 ± 0.5^{ab}	76.0 ± 0.4^{a}

Values within columns bearing the same small letter superscript(s) do not significantly differ at $p > 0.05$.

Table 3.4 Rapidly digested starch (RDS), slowly digested starch (SDS) and resistant starch (RS) content of spherulites formed in ethanol at 4°C (ES4), in water at 4°C (WS4), in water at 50°C (WS50) and in water from 50°C to 4°C (WS50-4), respectively.

Spherulites	RDS (%)	SDS (%)	RS (%)
ES4	19.6±0.4[a]	27.8±0.8[a]	52.6±0.7[d]
WS4	11.8±0.4[c]	25.5±0.6[b]	62.8±0.9[b]
WS50	15.8±0.7[b]	24.0±0.5[b]	60.0±0.2[c]
WS50-4	15.1±0.4[b]	11.9±0.1[c]	73.0±0.3[a]

Values within columns bearing the same small letter superscript(s) do not significantly differ at $p > 0.05$.

Table 3.5 Thermal properties of samples formed in ethanol at 4°C (ES4), in water at 4°C (WS4), in water at 50°C (WS50) and in water from 50°C to 4°C (WS50-4), respectively.

Samples	T_o (°C)	T_p (°C)	T_c (°C)	ΔH (J/g)
ES4	56.4±0.8^{d}	81.4±0.1^{d}	105.0±0.6^{c}	22.4±0.6^{d}
WS4	59.8±0.8^{c}	82.7±0.2^{c}	108.1±0.3^{c}	25.6±0.8^{c}
WS50	67.4±0.2^{a}	114.5±0.3^{b}	139.8±0.9^{b}	33.4±0.9^{b}
WS50-4	62.8±0.6^{b}	116.2±0.5^{a}	147.6±0.8^{a}	47.2±0.8^{a}

Values within columns bearing the same small letter superscript(s) do not significantly differ at $p > 0.05$.

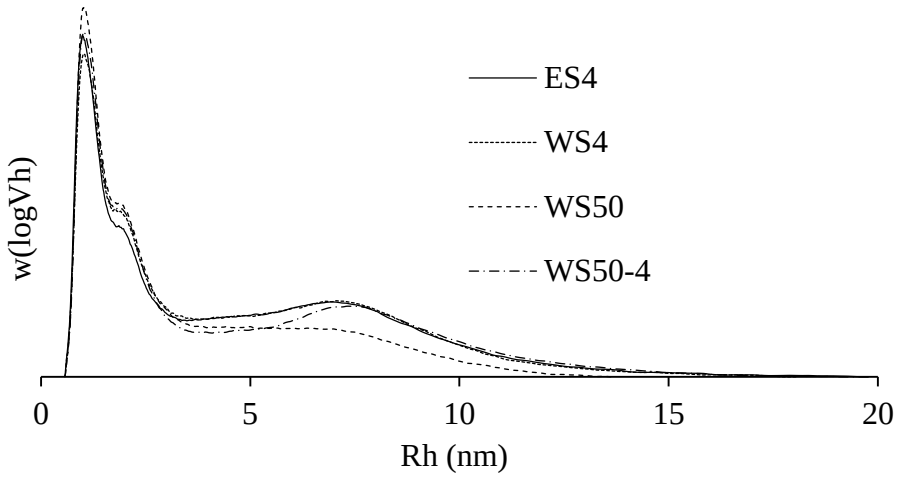

Figure 3.1 Molecular size distribution of spherulites formed in ethanol at 4 °C (ES4), in water at 4°C (WS4), in water at 50°C (WS50) and in water from 50°C to 4°C (WS50-4).

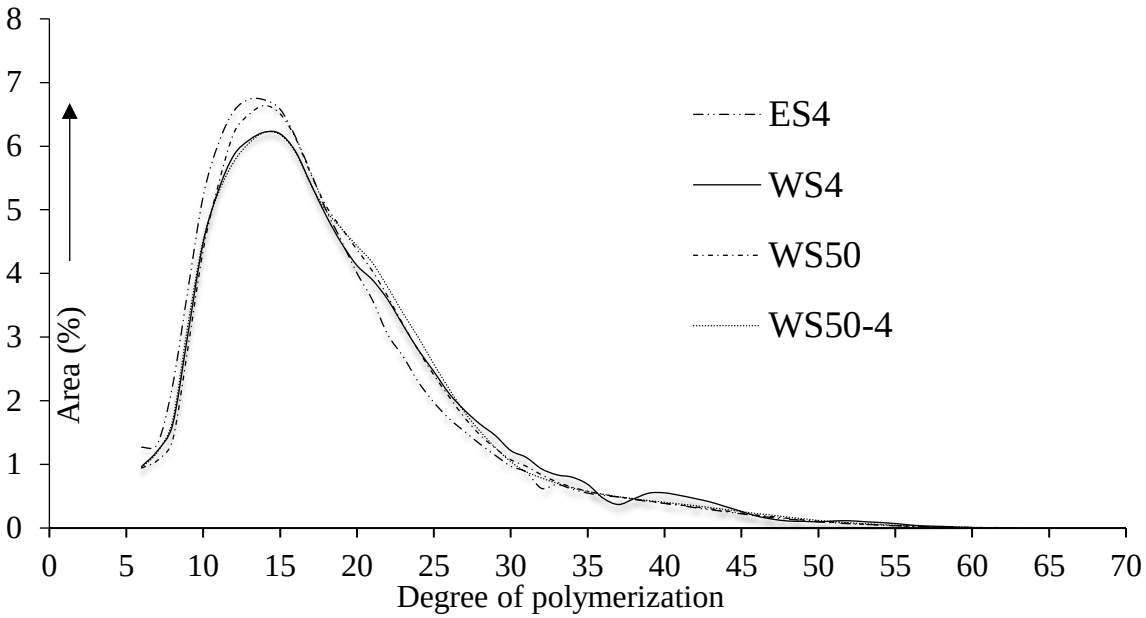

Figure 3.2 Chain length distribution of spherulites formed in ethanol at 4°C (ES4), in water at 4°C (WS4), in water at 50°C (WS50) and in water from 50°C to 4°C (WS50-4).

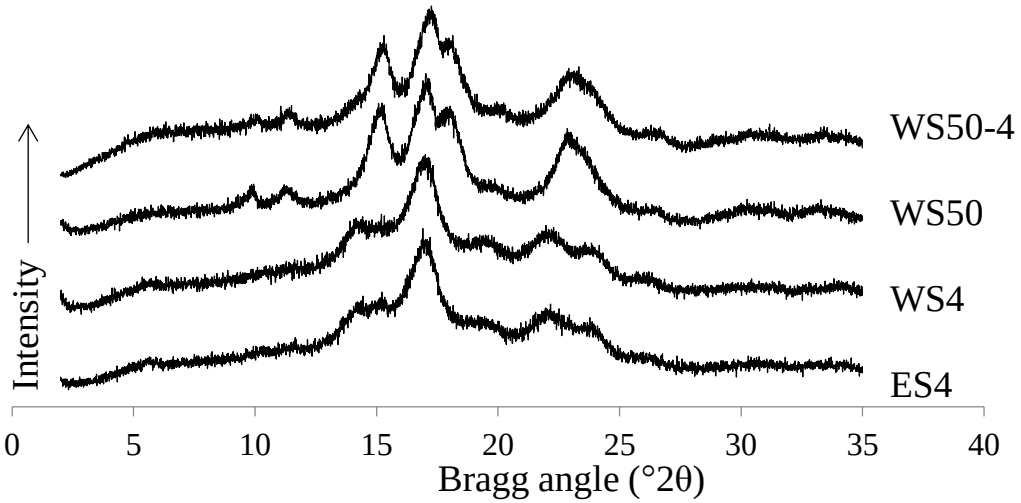

Figure 3.3 X-ray diffraction of spherulites formed in ethanol at 4°C (ES4), in water at 4°C (WS4), in water at 50°C (WS50) and in water from 50°C to 4°C (WS50-4).

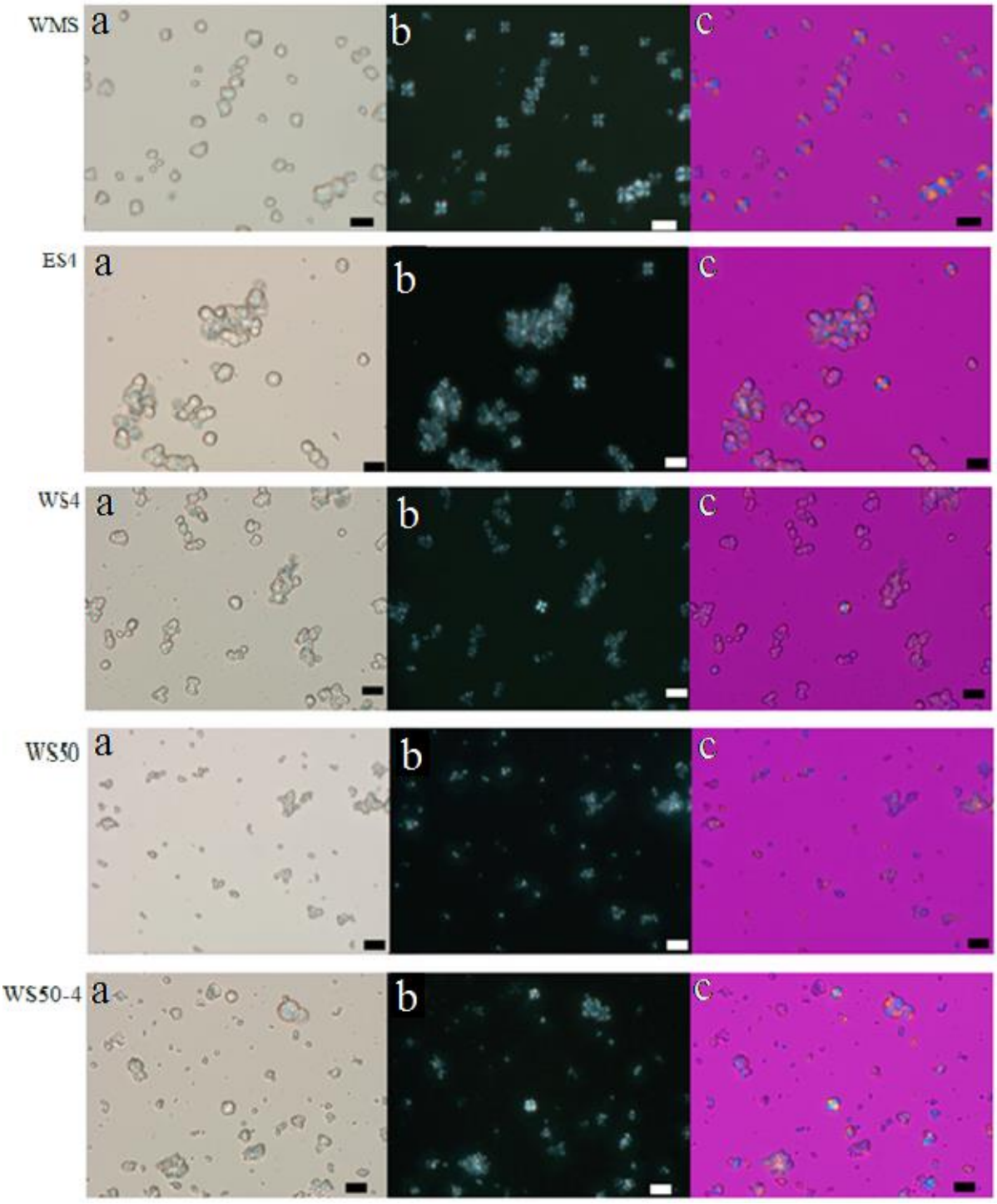

Figure 3.4 Microscopic images of waxy maize starch (WMS), and spherulites formed in ethanol at 4°C (ES4), in water at 4°C (WS4), in water at 50°C (WS50), and in water from 50°C to 4°C (WS50-4), under normal light (a), polarized light (b), and a combination of polarized light and wave plate (c). Each scale bar equals 20μm.

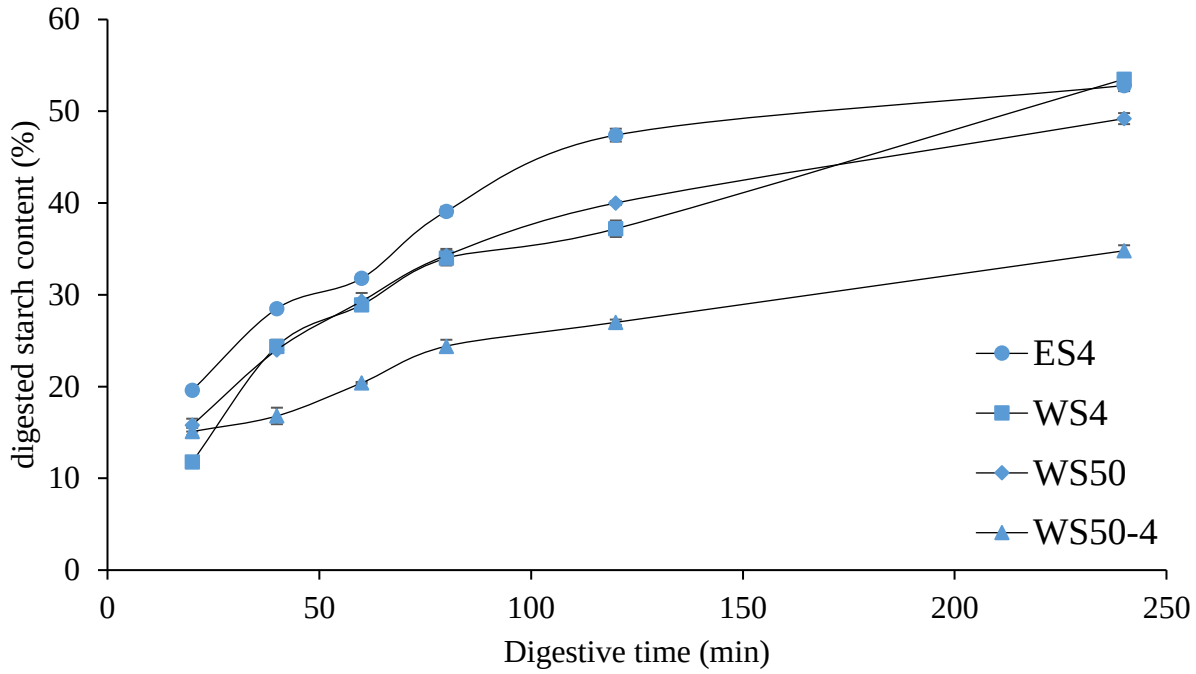

Figure 3.5 Digestibility of spherulites formed in ethanol at 4°C (ES4), in water at 4°C (WS4), in water at 50°C (WS50) and in water from 50°C to 4°C (WS50-4).

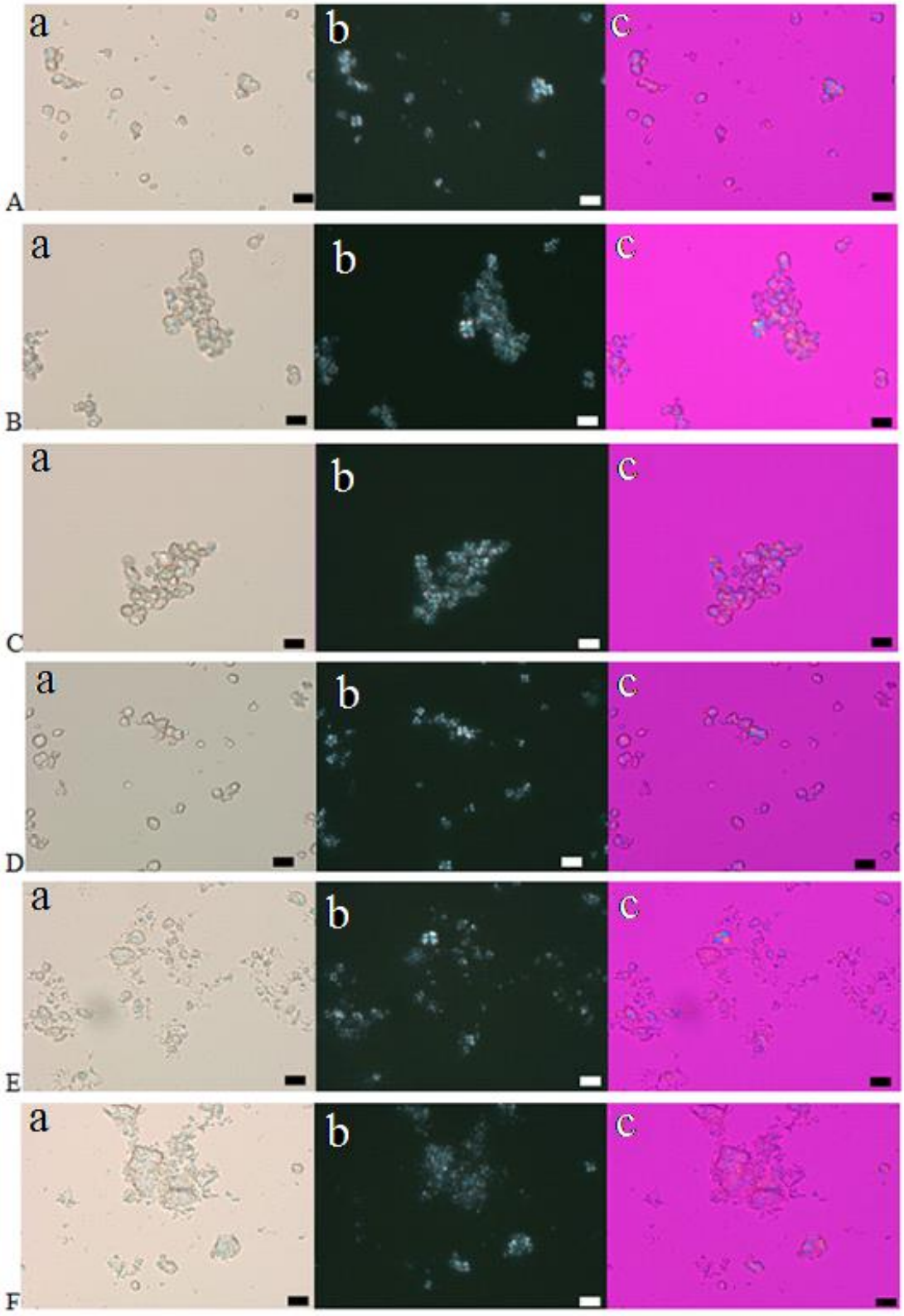

Figure 3.6 Microscopic images of enzyme resistant residues from the spherulites formed in ethanol at 4°C (ES4) at the digestion time of 20 (A), 40 (B), 60 (C), 90 (D), 120 (E), and 240 min (F), under normal light (a), polarized light (b), and a combination of polarized light and wave plate (c). Each scale bar equals 20μm.

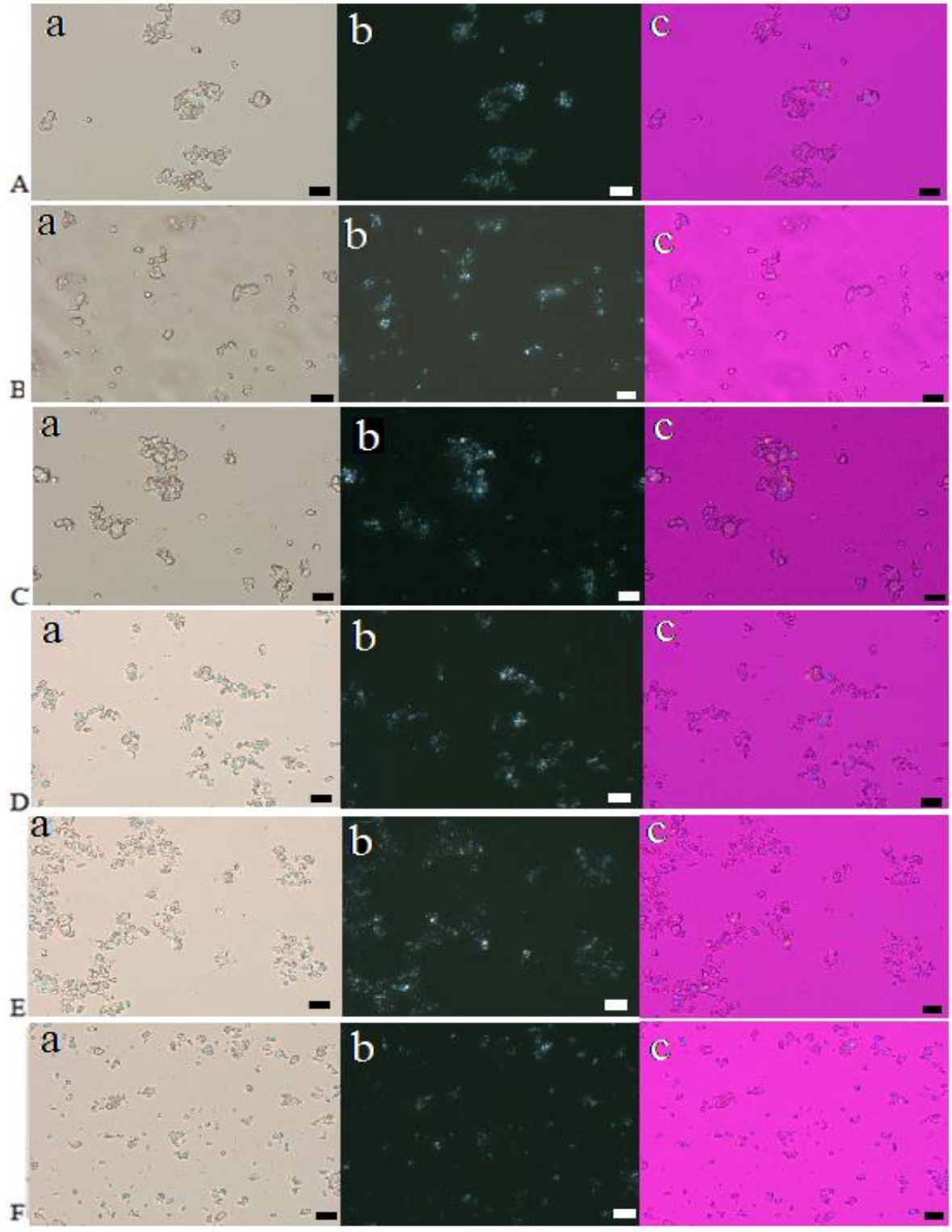

Figure 3.7 Microscopic images of enzyme resistant residues from the spherulites formed in water at 4°C (WS4) at the digestion time of 20 (A), 40 (B), 60 (C), 90 (D), 120 (E), and 240 min (F), under normal light (a), polarized light (b), and a combination of polarized light and wave plate (c). Each scale bar equals 20μm.

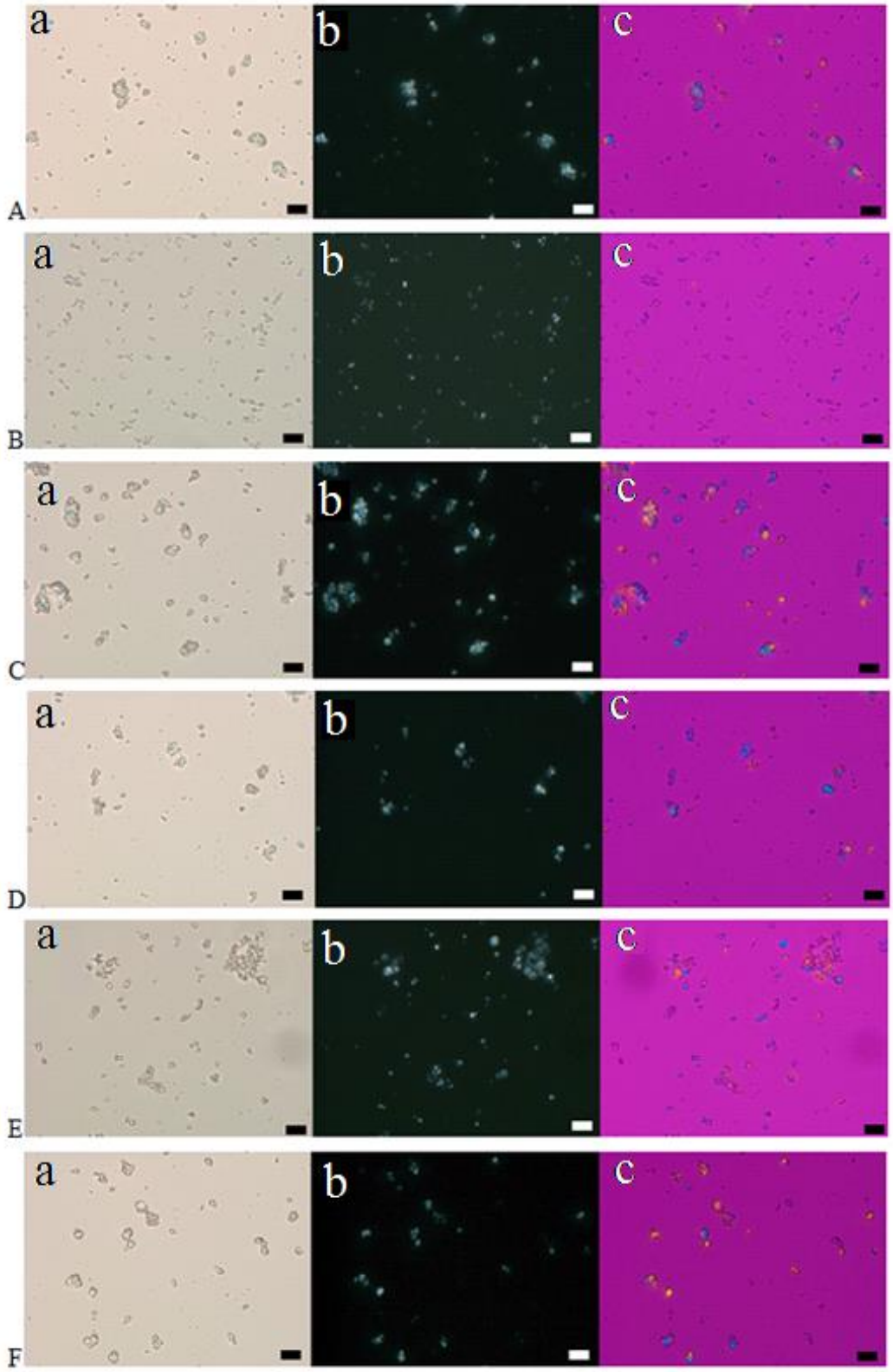

Figure 3.8 Microscopic images of enzyme resistant residues from the spherulites formed in water at 50°C (WS50) at the digestion time of 20 (A), 40 (B), 60 (C), 90 (D), 120 (E), and 240 min (F), under normal light (a), polarized light (b), and a combination of polarized light and wave plate (c). Each scale bar equals 20μm.

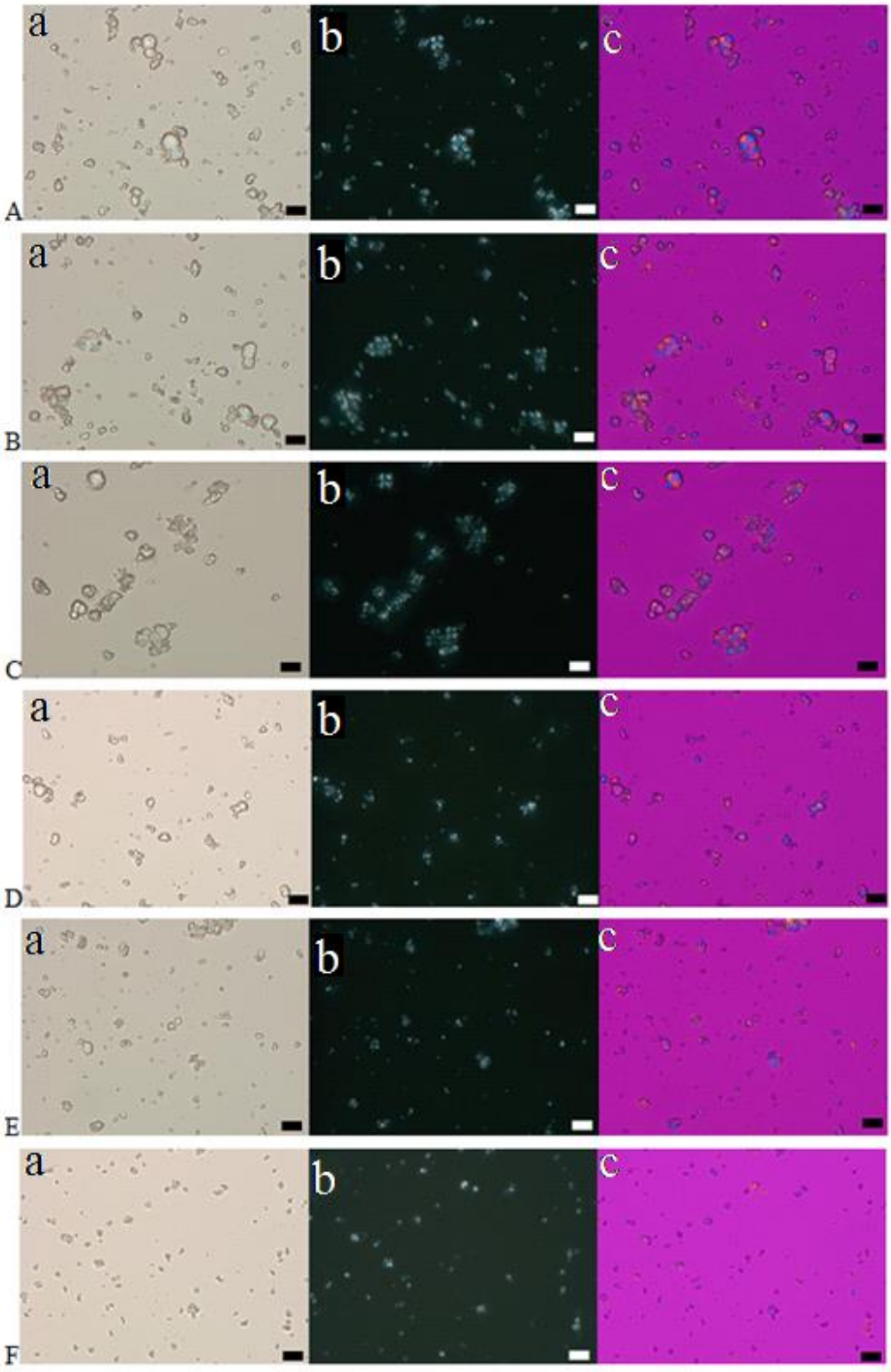

Figure 3.9 Microscopic images of enzyme resistant residues from the spherulites formed in water from 50°C to 4°C (WS50-4) at the digestion time of 20 (A), 40 (B), 60 (C), 90 (D), 120 (E), and 240 min (F), under normal light (a), polarized light (b), and a combination of polarized light and wave plate (c). Each scale bar equals 20μm.

Chapter 4 - Conclusions and Perspectives

The effects of three pullulanase activity levels on debranching of waxy maize starch were compared in this study. After 24 hours of debranching and 24 hours of crystallization, the samples treated by different levels of pullulanase activity levels had similar precipitate yield, even though higher pullulanase resulted into more debranched material. When the pullulanase activity was increased to 240 NPUN/g, more than 80% starch was debranched. The degree of crystallinity and the RS content were also increased with higher pullulanase activity levels. After the debranched starches were crystallized at 25°C for 24 h, the RS content was greater than 63%.

The sample treated by 80 NPUN/g of pullulanase was used to produce spherulites. After heating to 183°C and cooling to 4 or 50°C in water, the morphology of crystallized material was different. When the sample was cooled to 4°C, 45° rotated Maltese cross was observed; but when the crystallization temperature was 50°C, no Maltese cross was observed. When these samples crystallized at 50°C were further crystallized at 4°C, some particles showed “positive” Maltese cross. The RS content and degree of crystallinity were highest in sample WS50-4. The RS contents in WS4 and WS50 were 62.8% and 60.0%, but the degree of crystallinity in sample WS50 was higher. WS50 and WS50-4 were A-type crystallites. With adding ethanol, “positive” spherulites were produced, but the RS content was the lowest. After crystallization, ES4 and WS4 have similar degree of crystallinity and both of them were B-type crystallites.

In the future, the debranched starch treated by the other two levels of pullulanase will be also used to produce spherulites. Since the formation of crystalline is influenced by chain length, the RS content, degree of crystallinity, types of crystallites and morphology need to be investigated and the results will be helpful to determine the relationship between digestibly and structures.

Appendix A - Nelson/Somogyi reducing sugar method regent preparation

Solution A was made by dissolving 2.5 g anhydrous sodium carbonate, 2.5 g sodium potassium tartrate and 20 g sodium sulfate in 100 ml de-ionized water. Solution B was made by dissolving 7.5g copper sulfate pentahydrate and a drop of concentrated sulfuric acid in 50 ml de-ionized water. Copper regent was made by mixing 25 ml solution A and 1 ml solution B. Solution C was made by dissolving 5 g ammonium molybdate, 4.2 ml concentrated sulfuric acid and 0.6 g disodium hydrogen arsenate heptahydrate in 100 ml water. Arsenomolybdate regent was made by diluting solution C to 500 ml (McCleary, 1999).

Appendix B – Modified Englyst's method for starch digestion

For each sample, starch (600 mg) and guar gum (50 mg) were weighed into a 45 ml centrifuge tube containing 10 ml 0.05 M hydrochloric acid. Pepsin was not used as samples were devoid of protein. The tube was incubated in 37°C water bath for 30 min. Then, 10 ml 0.25M sodium acetate buffer and 30 glass beads were added. Enzyme solution was prepared using 3 g pancreatin (P7545, sigma) in 20 ml water and stirred for 10 min, then centrifuged at 1750 ×g for 10 min. A 15 ml portion of the supernatant was mixed with 1.7 ml water containing 60 mg amyloglucosidase (20300 units/g). This enzyme solution (5 ml) was added into the tube containing the acidified starch and the starch was incubated in 37°C water bath for 20, 40, 60, 90, 120 and 240 min. At each time point, 4 ml of mixture in centrifuge tube was transferred into 20 ml 66% ethanol solution and mixed well. A 0.1 ml aliquot of ethanol mixture was diluted to 1 ml for glucose measurement (Englyst et al., 1992; Sang & Seib, 2006).

Appendix C – The degree of crystallinity calculation

The X-ray data is exported in excel format. The curve is plotted with Orgin Lab 8.5. In order to calculate the relative degree of crystallinity, a straight base line is created and subtracted by the curve. Click "multiple peak fit" and select the peak type as "Gauss". Select the peak number as 2, 3, or 4, until the most fitted gauss peak can be obtained. The most fitted gauss peak should fit in the curve without crossing the majority peaks area. The area of gauss peak (A_a) represents the content of amorphous portion, and the area value is given after plotting the gauss peak. The area between the curve and the gauss peak (A_c) indicates the portion of crystallites. The total area between the curve and baseline $A_t = A_a + A_c$. Select the curve and click "integrate", the value of A_t will be given. The degree of crystallinity can be calculated based on the following equation: degree of crystallinity = $A_c/A_t = (A_t - A_a)/A_t$ (Komiya & Nara, 1986).

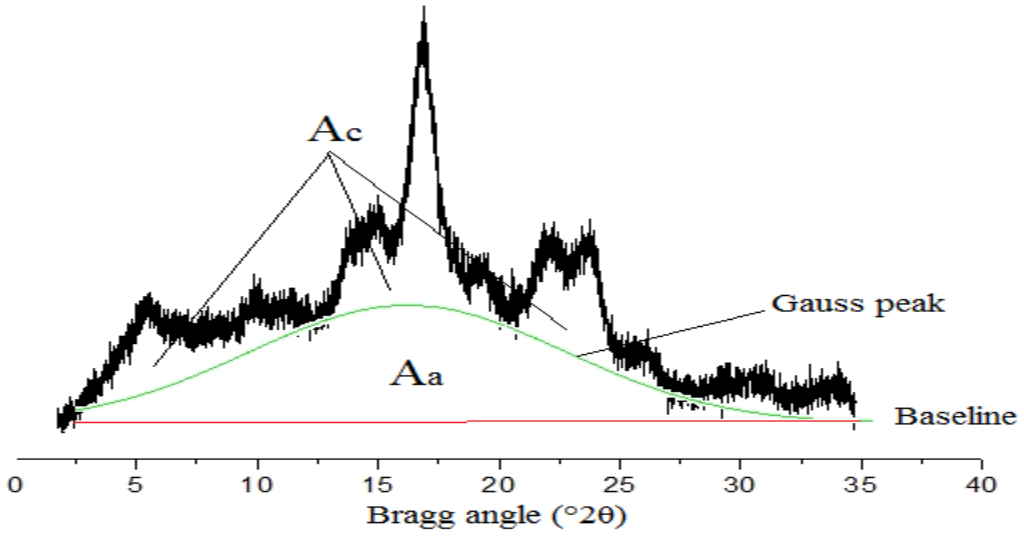

Appendix D – The procedure of DSC analysis

The DSC data is analyzed with TA Universal Analysis, and the curve of a sample as below. When temperature increases, a peak can be detected. Click “integrate peak linear” and set a point at the beginning of this peak and another point at the end of this peak, press “enter”, the onset temperature, peak temperature and enthalpy will be shown. Right click on the end point of the peak, and click the temperature at that point, the conclusion temperature can be given.